



Climate variability and Change in South America from WCRP/CMIP3 (IPCC-AR4) simulations

Carolina Vera

**CIMA, Universidad de Buenos Aires,
Buenos Aires, Argentina**



Outline

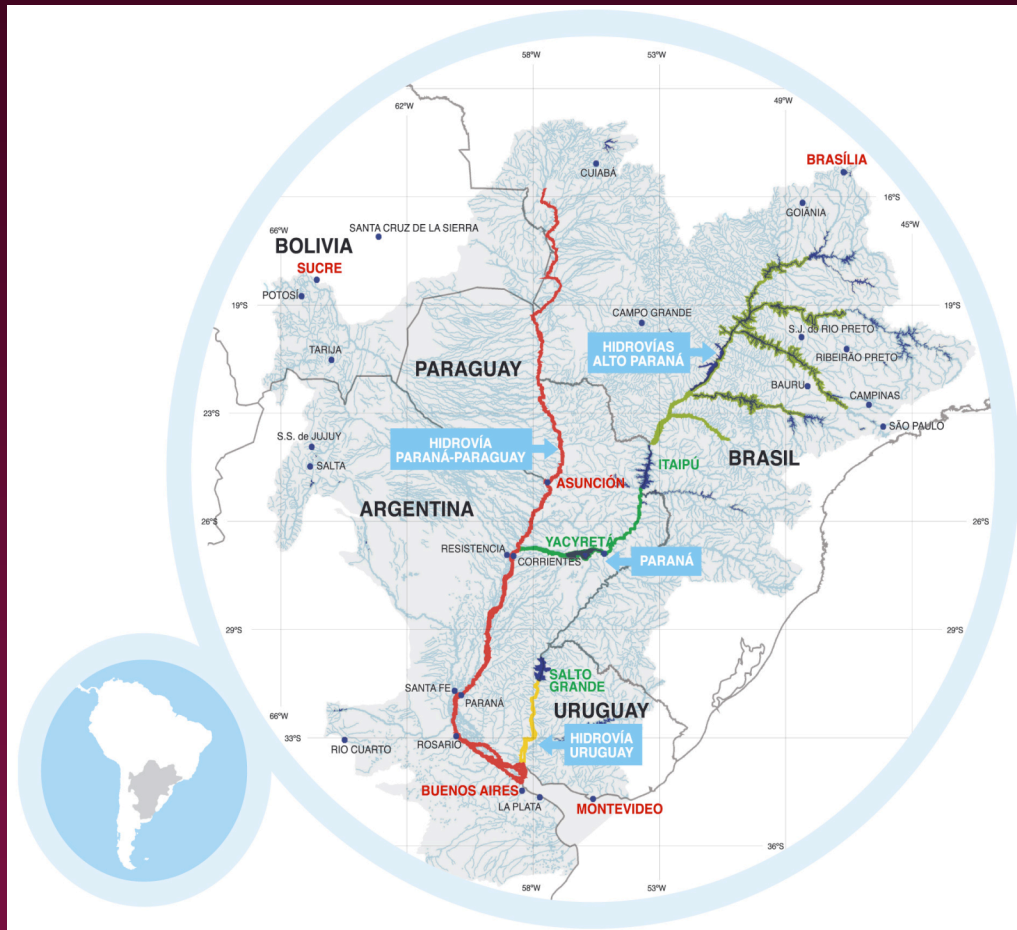
- Brief description of the main features regarding:
 - Seasonal Cycle
 - MCS activity
 - Intraseasonal Variability
 - Interannual Variability
 - Long-term observed trends
 - Climate change projections

Including:

- Discussion of current level of understanding focusing on the multi-scale nature of the problem
- Discussion of modeling current ability in describing those features

Focus on the La Plata Basin (LPB) region

The La Plata Basin



- The Plata Basin covers about 3.6 million km².

- The La Plata Basin is the fifth largest in the world and second only to the Amazon Basin in South America in terms of geographical extent.

- The principal sub-basins are those of the Parana, Paraguay and Uruguay rivers.

- The La Plata Basin covers parts of five countries, Argentina, Bolivia, Brazil, Paraguay and Uruguay.

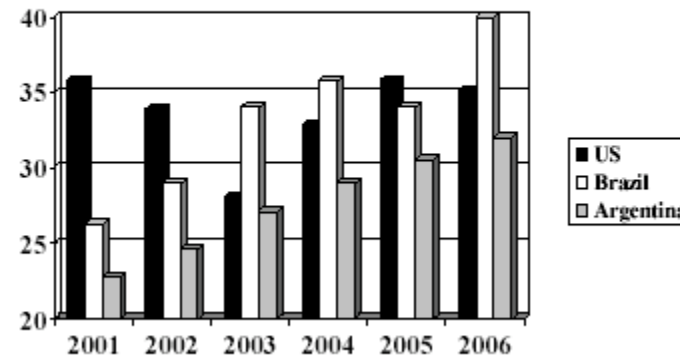
Global relevance of the la Plata Basin



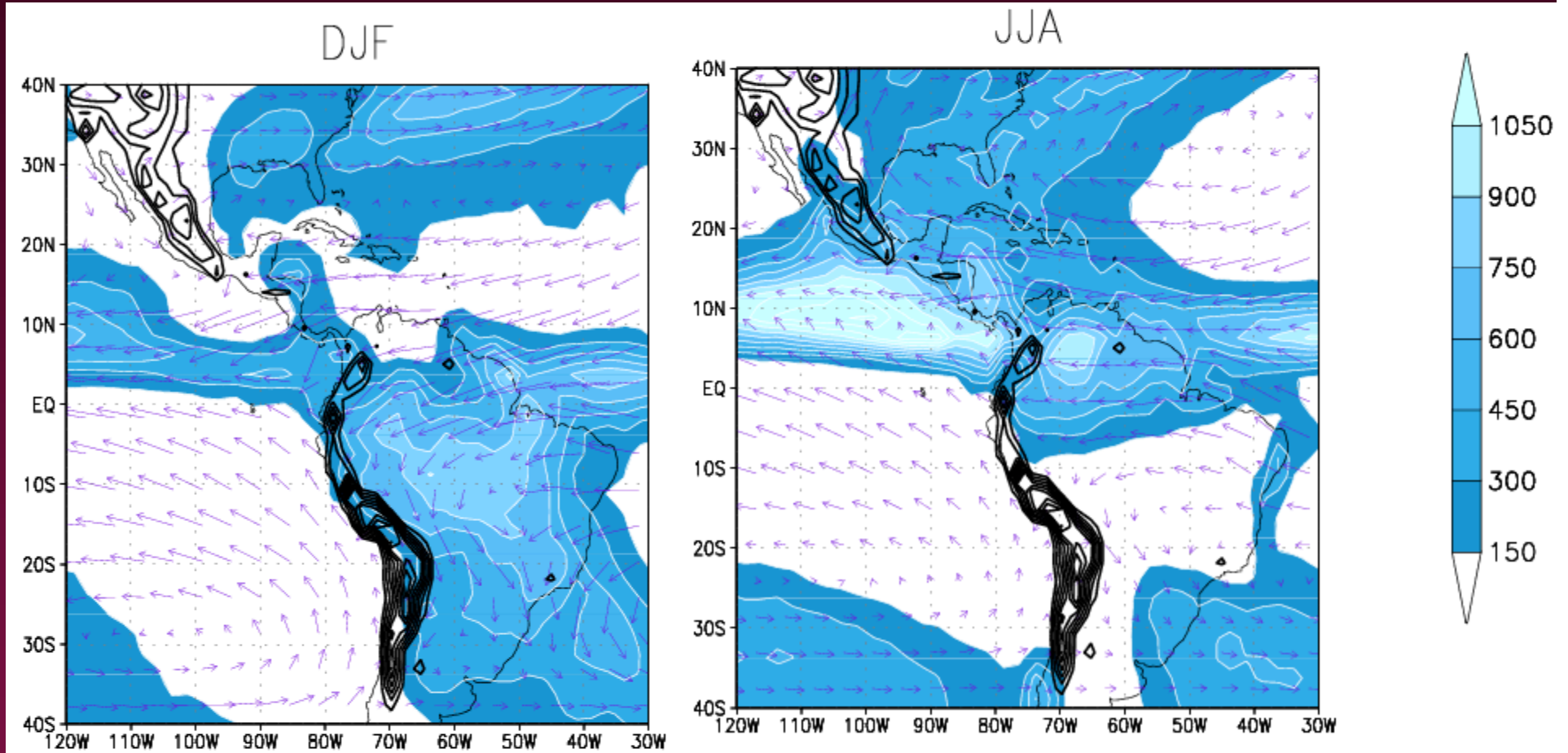
- LPB is home of more than 100 million people including the capital cities of 4 of the five countries, generating 70% of the five countries GNP.
- The fluvial transport of the Paraguay-Paraná Waterway was of 13,000,000 tons in 2004.
- The hydroelectric potential is estimated at 92,000 MW. There is more than 150 dams, and 60% of the hydroelectric potential is already used.
- It is one of the largest food producers (cereals, soybeans and livestock) of the world.



Export of Soybeans/Meal
US, Brazil, Argentina - MMT



Climatological seasonal means

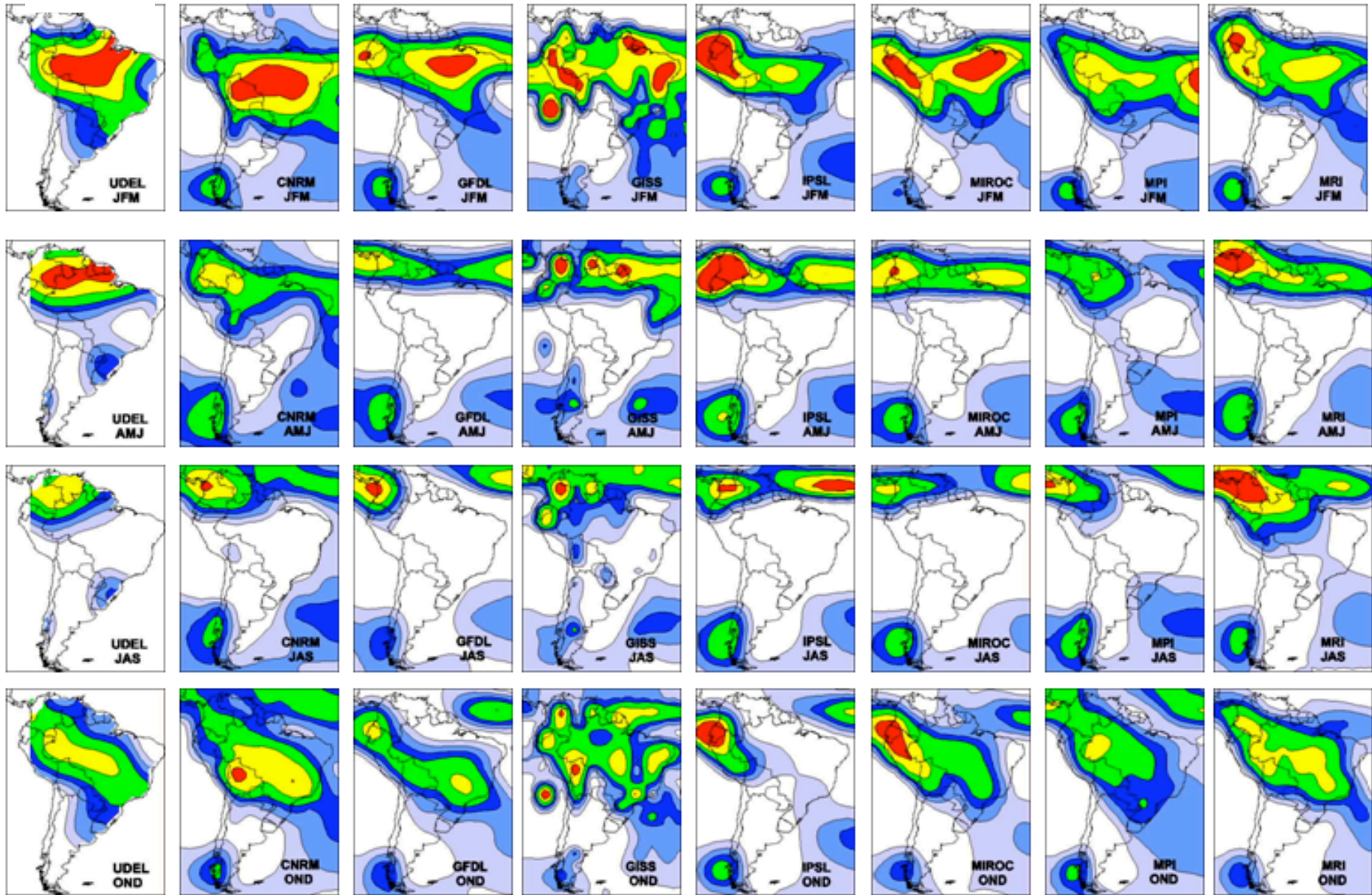


Climatological seasonal mean precipitation
(shaded, NCEP reanalysis), & vertically
integrated moisture fluxes (arrows, CMAP)

(Vera et al., 2006, J. Climate)

Seasonal Cycle of precipitation from WCRP/CMIP3 models

OBS



(1970-1999 period)

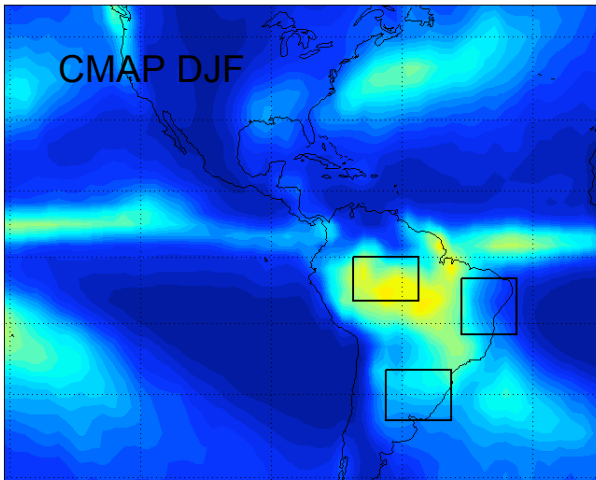
(Vera et al., 2006, GRL)

DEMETER assessment over South America

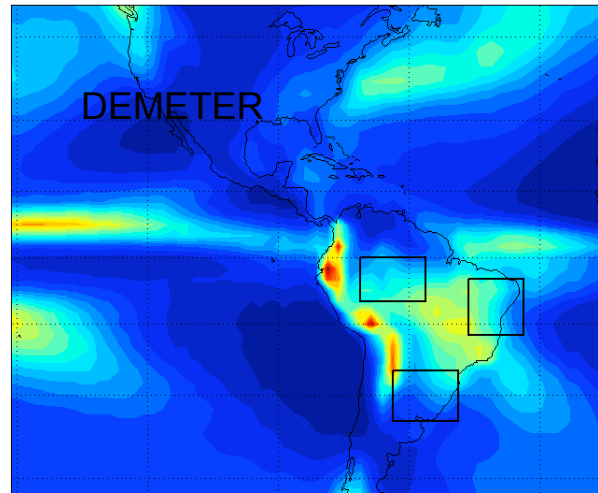
"Development of a European Multimodel Ensemble system for seasonal to interannual prediction"

Seasonal Precipitation

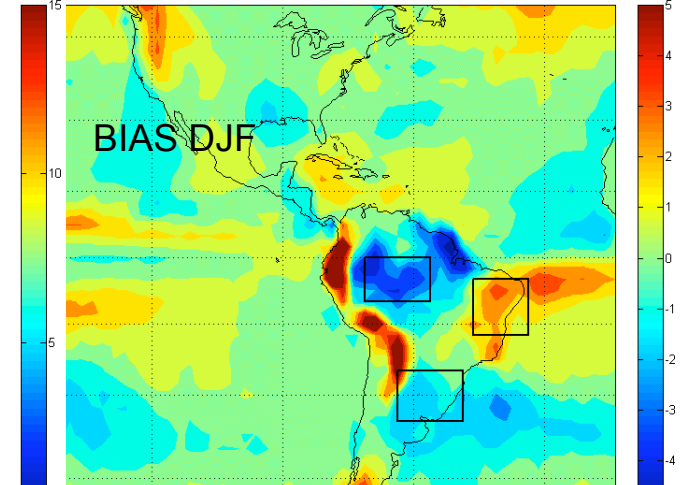
CMAP Precipitation for DJF in mm/day



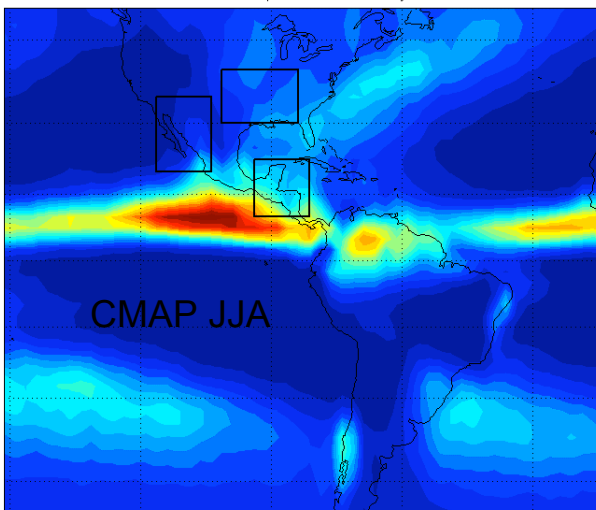
Multi-model hindcast for DJF precipitation (1991-2001 mean), mm/day



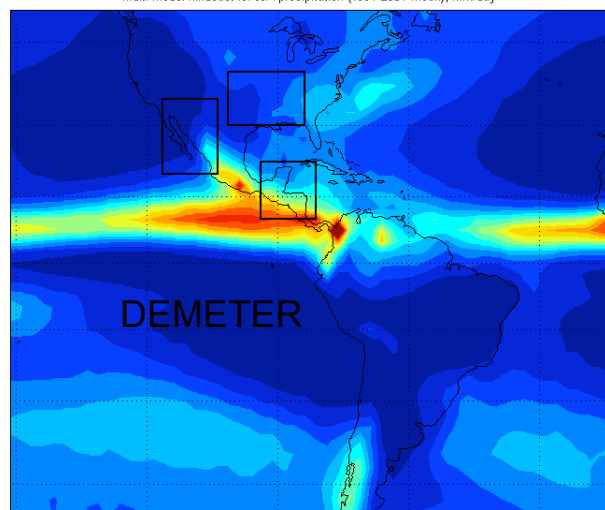
Bias between multi-model and CMAP Precipitation data for DJF (1991-2001 mean), mm/day



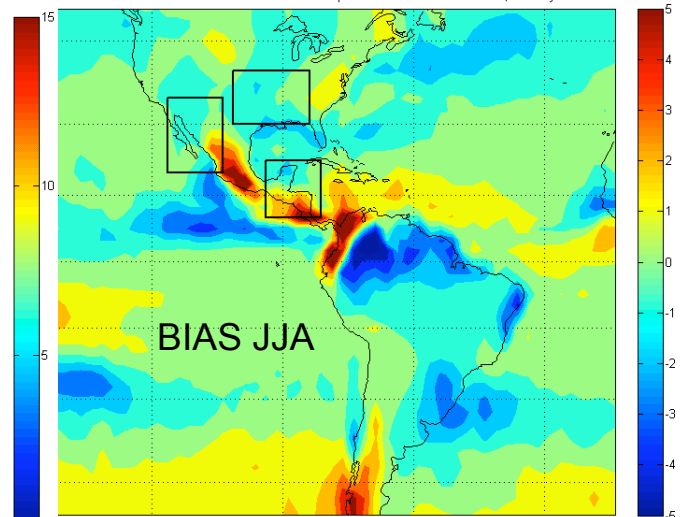
CMAP Precipitation for JJA in mm/day



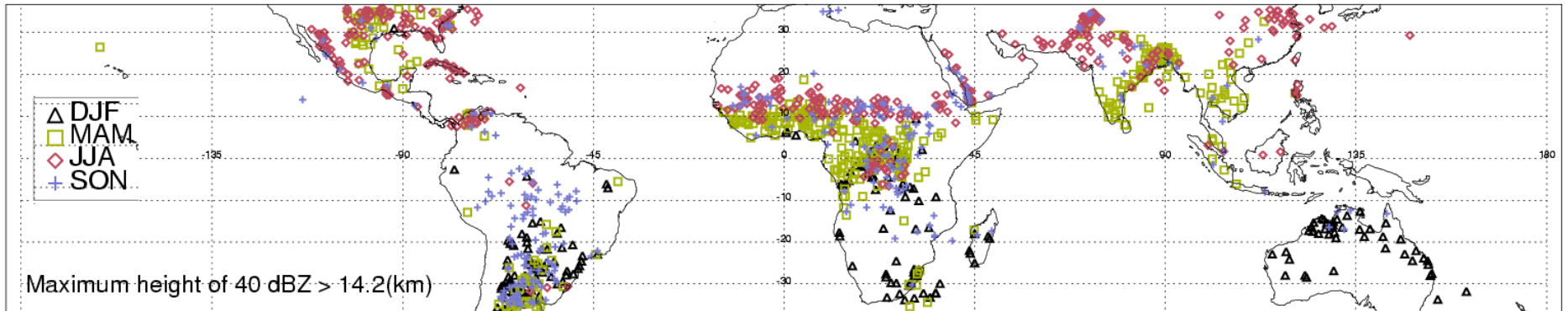
Multi-model hindcast for JJA precipitation (1991-2001 mean), mm/day



Mean bias between multi-model and CMAP Precipitation data for JJA 1991-2001, mm/day



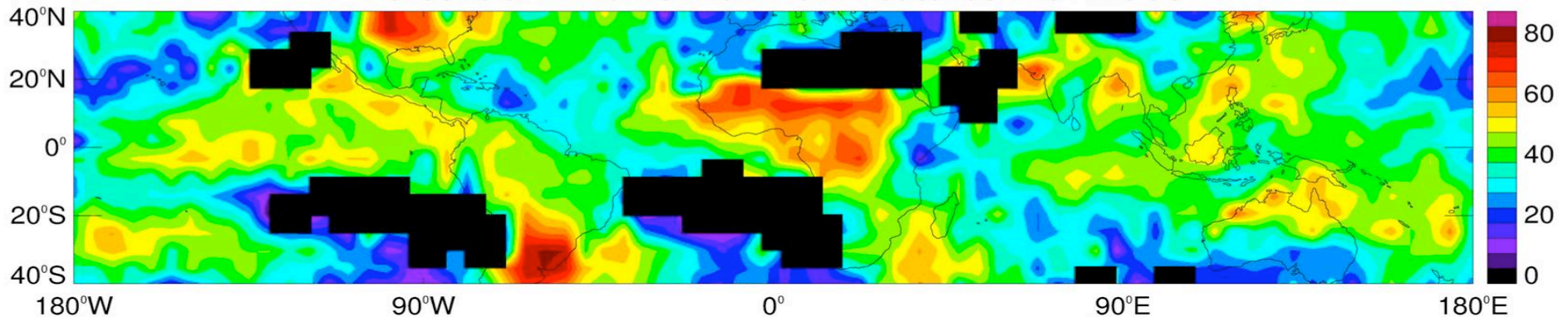
MCS activity in South America



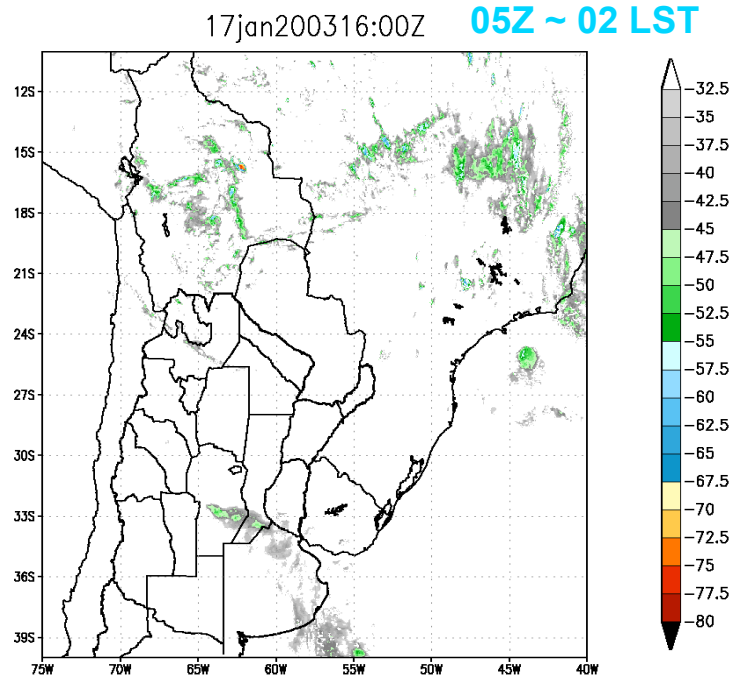
Subtropical South America has the largest fractional contribution of PFs with MCSs to rainfall of anywhere on earth between 36 N and 36 S

(Zipser et al. BAMS, 2006)

Percent of 2A25 Rainfall from Features with MCSs

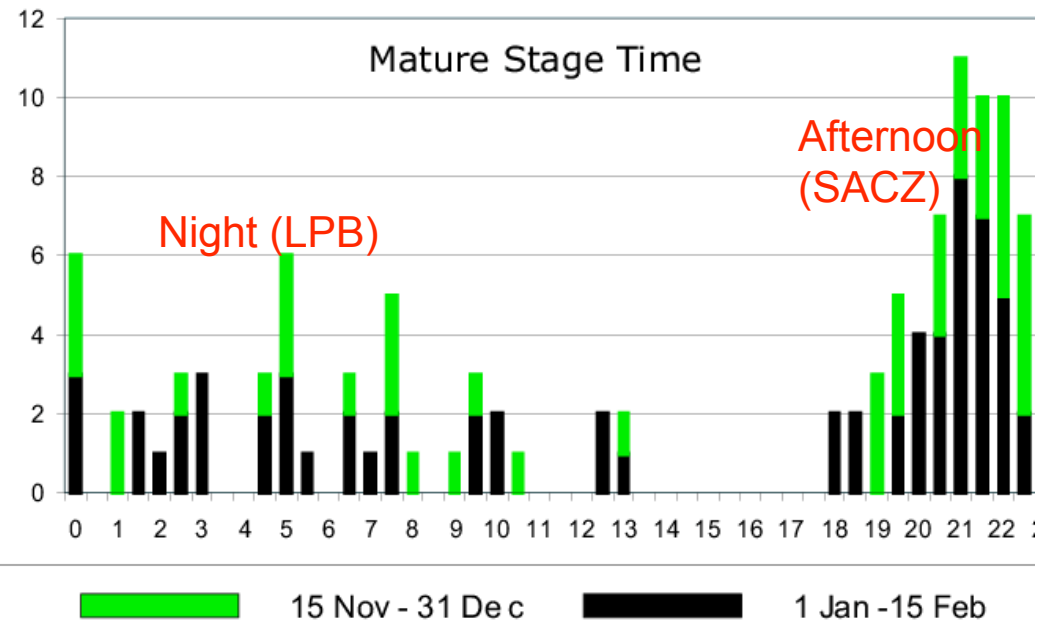


MCS activity in South America



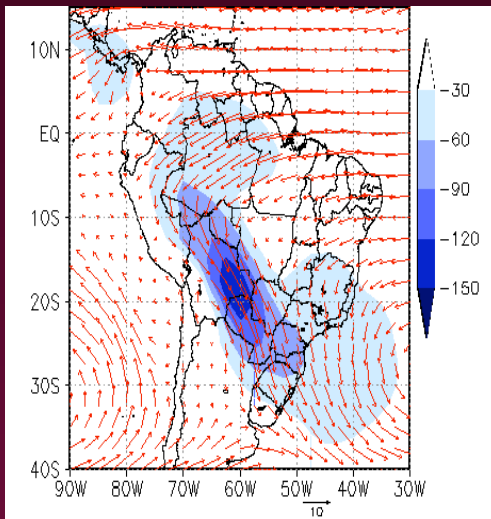
MCS event on 17 January 2003

MCS mature stage time occurrence frequency. Bars in green represent the period November 15 to December 31, in black January 1 to February 15 (Zipser et al. 2004)

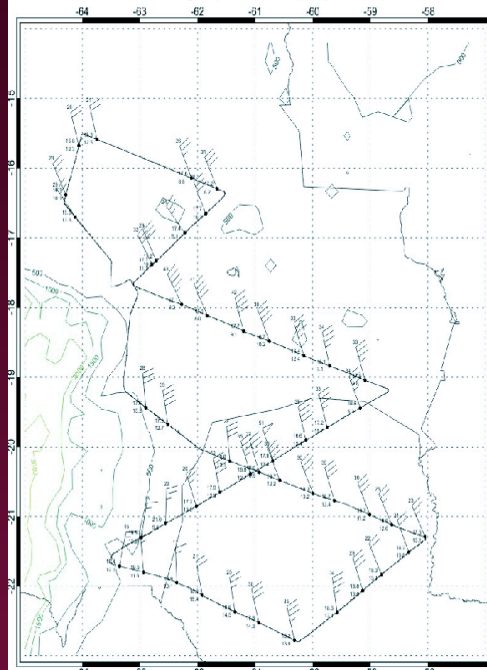


The South American Low-Level Jet

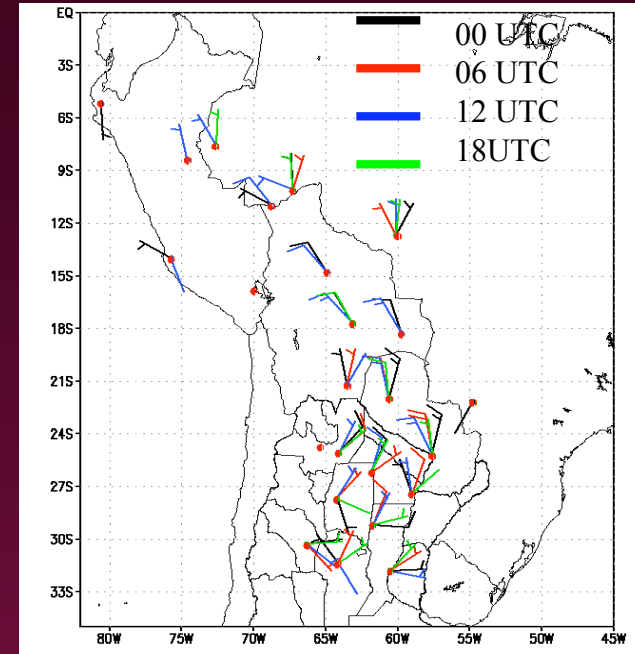
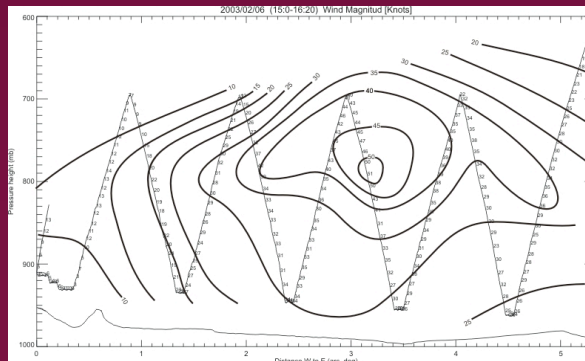
LLJ Composites NDJF,
(Marengo et al. 2004)



SALLJEX Flight (Level= 800_mb) 2003/02/06



SALLJ spatial structure
depicted by NOAA/P-3
missions in SALLJEX



SALLJ diurnal cycle
at 700 asl depicted
by SALLJEX
observations
(Nicolini et al. 2004)



MCS activity and the South American Low-Level Jet

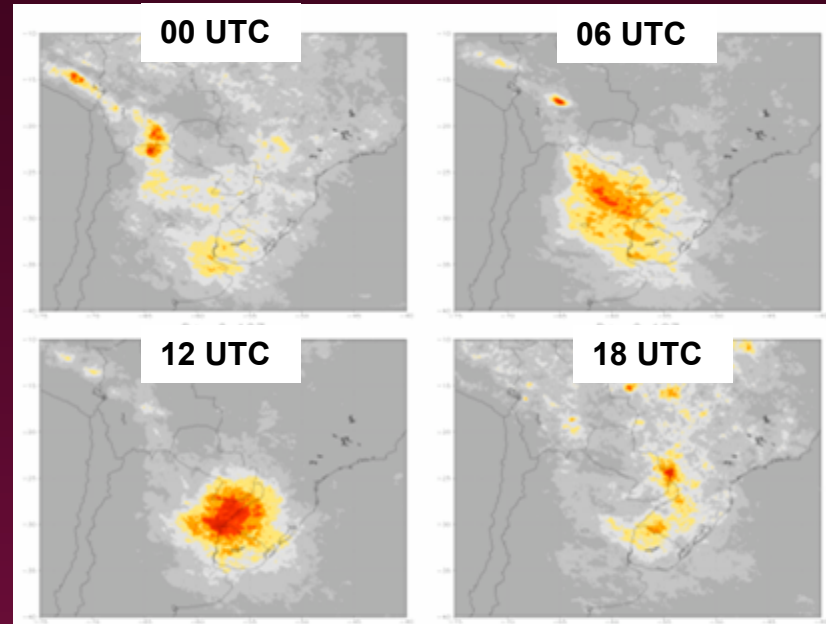
Frequency of Convection (2000-2003)

(Salio et al. MWR, 2007)

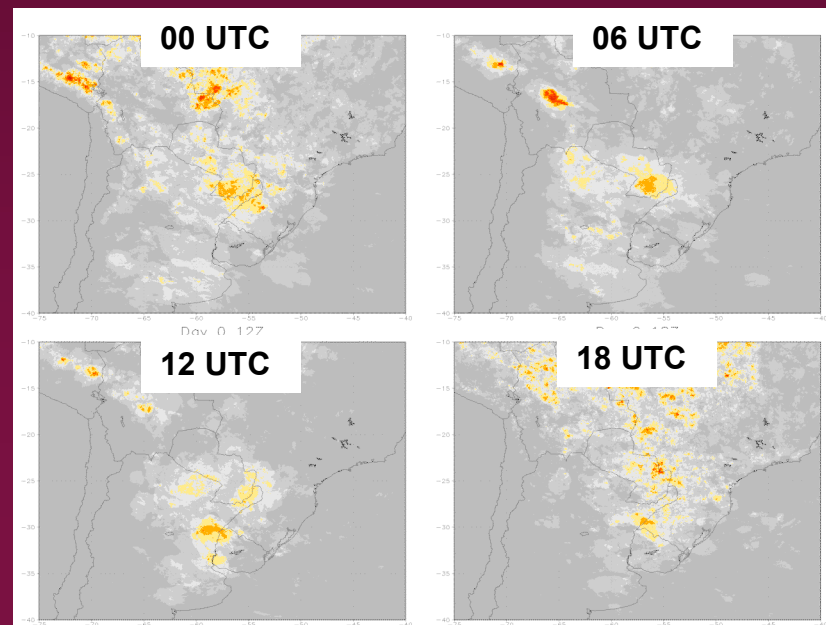
During SALLJ Days:

- Higher frequency of MCS occurrence (41%)
- Synoptic waves associated with SALLJ events provide the favorable environment for MCS development
- MCS are bigger and last longer

MCS tend to be nocturnal in both SALLJ and NO SALLJ dates over northern Argentina and Paraguay and diurnal over southern Brazil



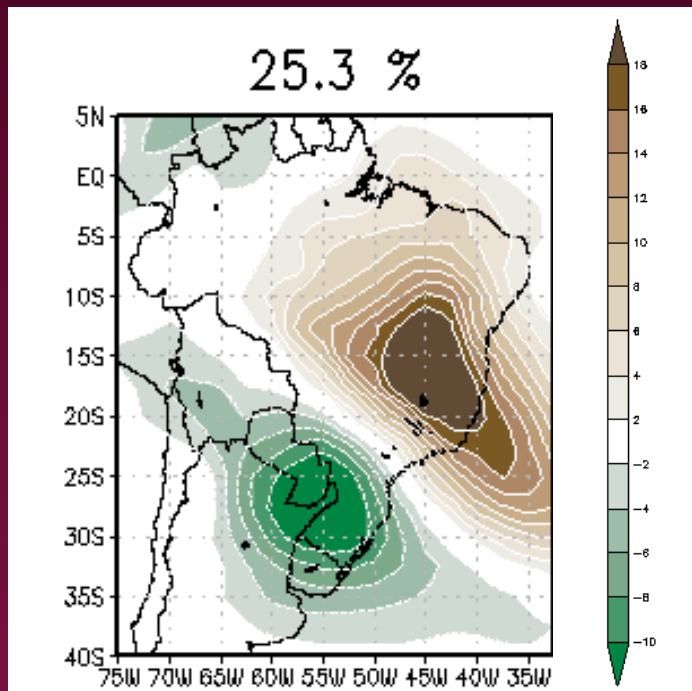
**SALLJ
Days**



**NO
SALLJ
Days**

Intraseasonal variability

1st EOF leading pattern of 10-90-day filtered OLR variability



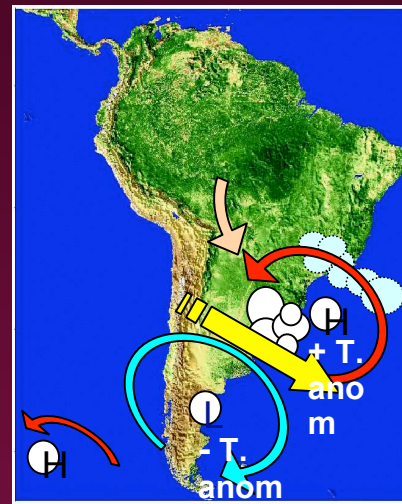
SOUTH AMERICAN SEE-SAW PATTERN

Nogues-Paegle and Mo (1997)

Diaz and Aceituno (2003)

Weakened SACZ

Intensified SALLJ
poleward progression



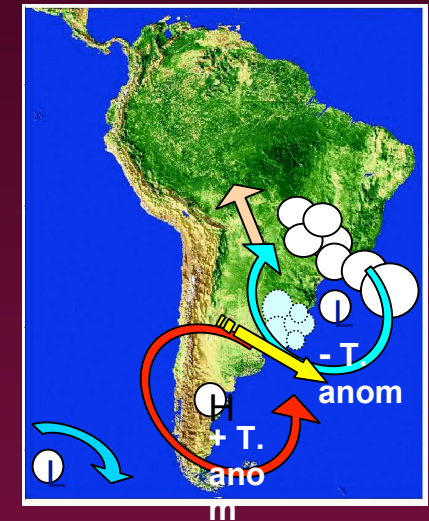
Higher frequency of extreme daily rainfall events at the subtropics

(Liebmann, Kiladis, Saulo, Vera, and Carvalho, 2004)

(Gonzalez, Vera, Liebmann, Kiladis, 2007)

Intensified SACZ

Inhibited SALLJ
poleward progression



Higher frequency of heat waves and extreme daily temperature events at the subtropics

(Cerme, Vera, and Liebmann, 2007)

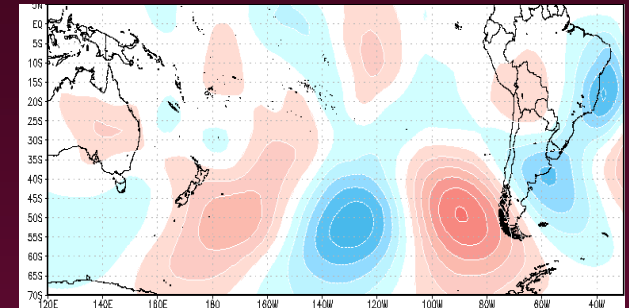
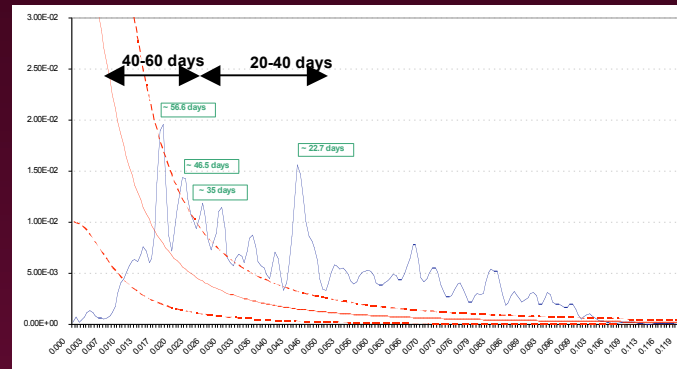
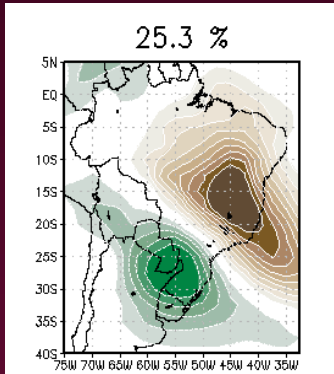
Intraseasonal variability from WCRP/CMIP3 Models

EOF-1 (10-90 days) Filtered OLR

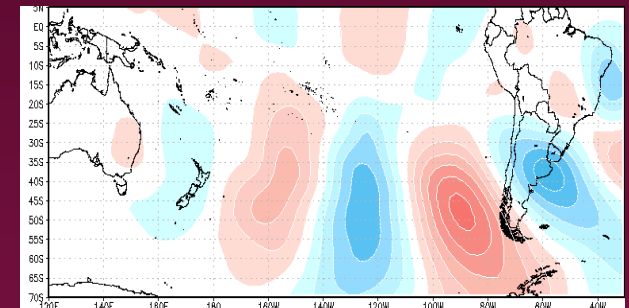
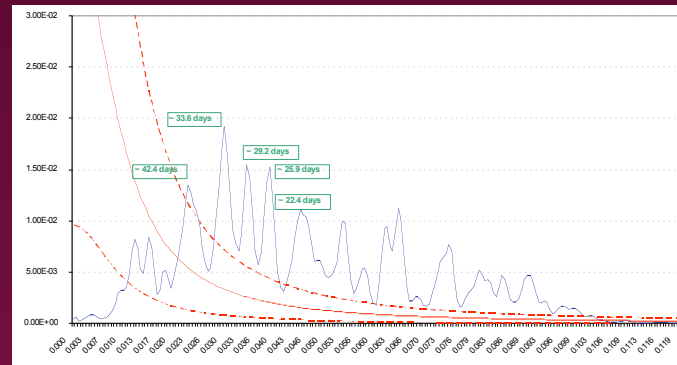
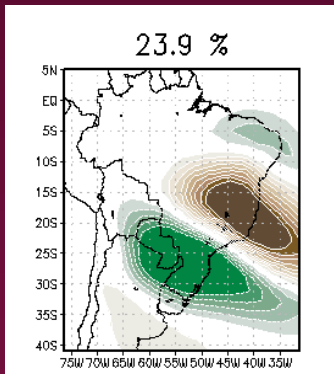
EOF-1 Spectral Density

Regressions EOF-1 & 200-hPa v'

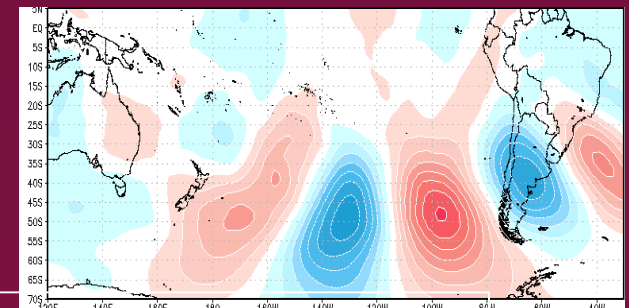
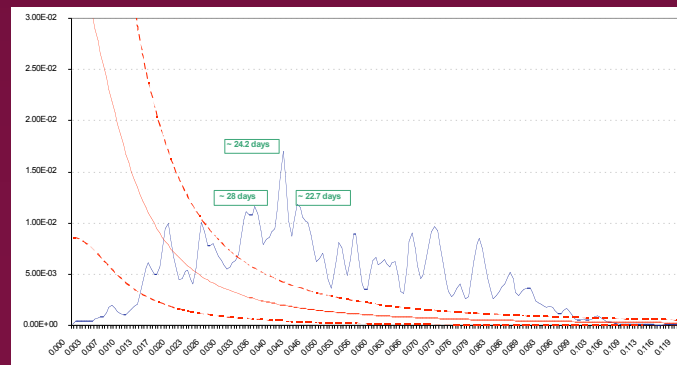
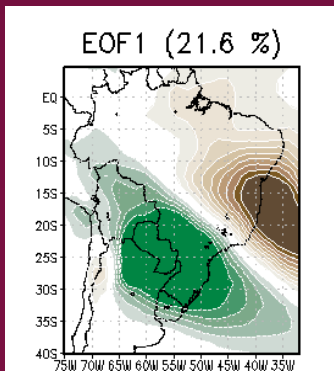
OBS



GFDL



MPI



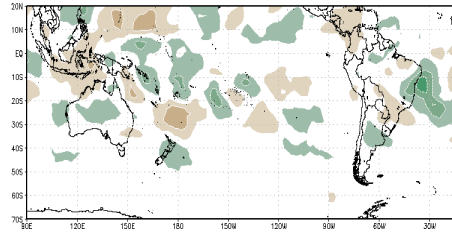
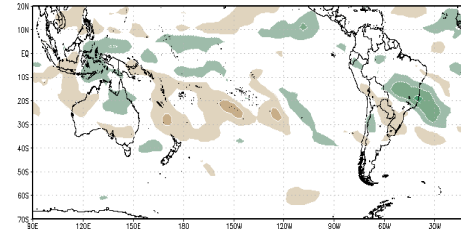
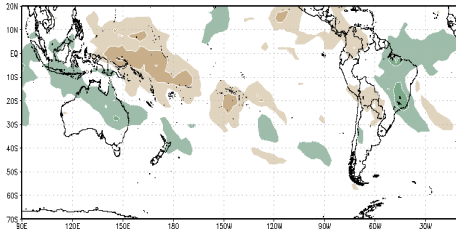
González, Vera, Carril (2007)

OBS

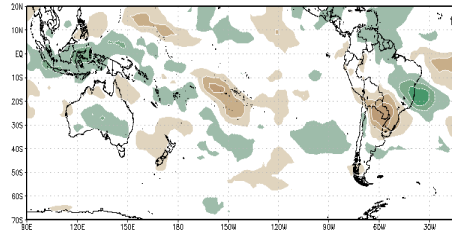
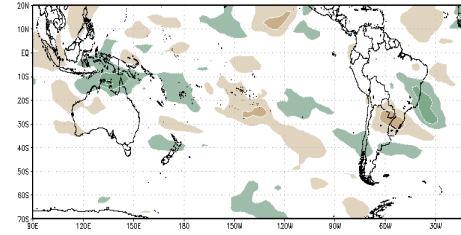
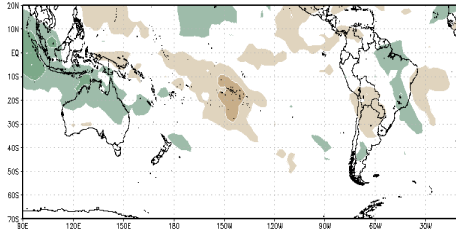
GFDL

MPI

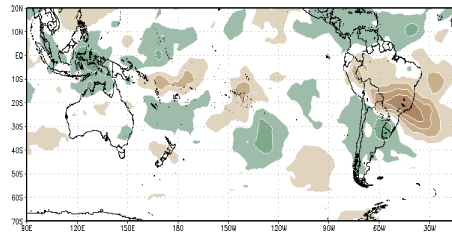
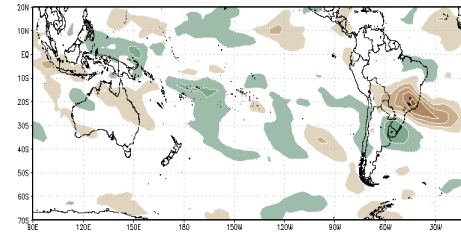
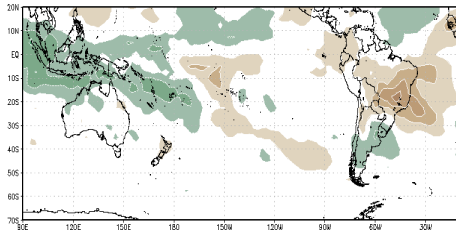
LAG -15



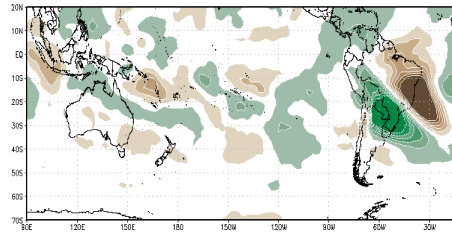
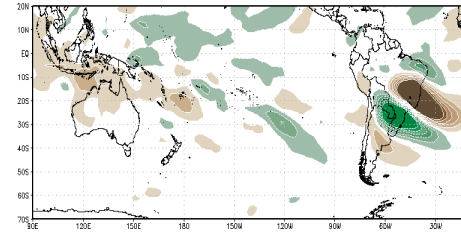
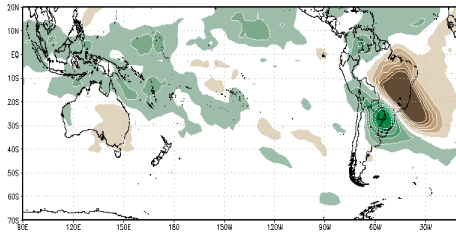
LAG -10



LAG -5



LAG 0



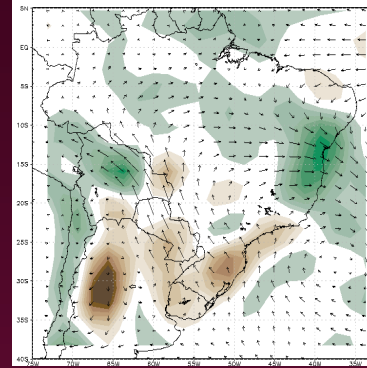
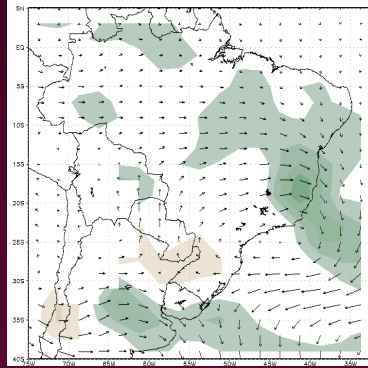
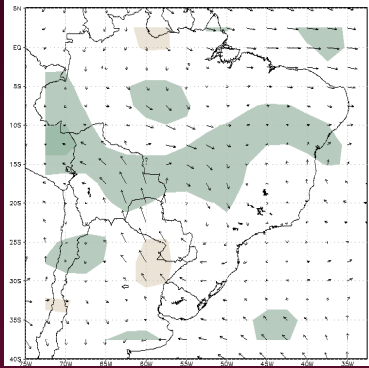
**Regressions
EOF-1 & OLR'**

NCEP/NCAR

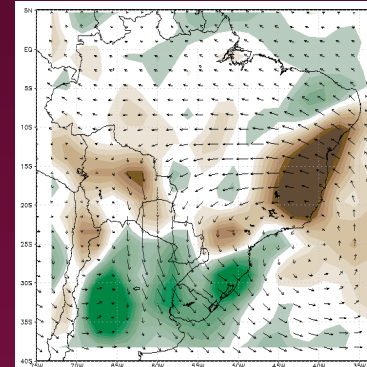
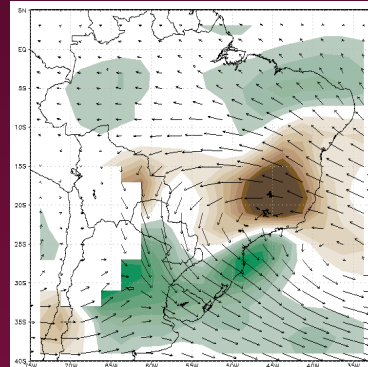
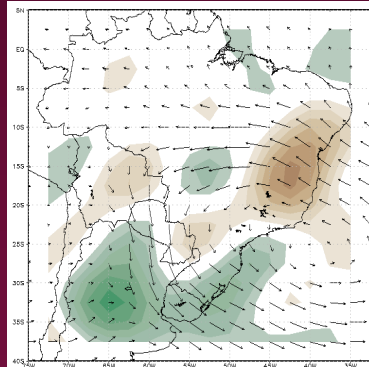
GFDL

MPI

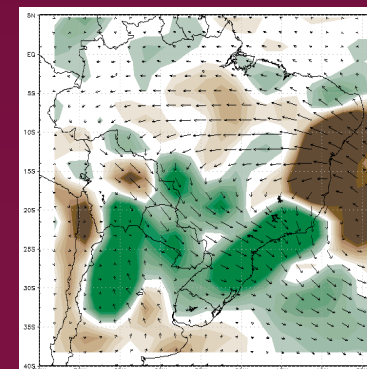
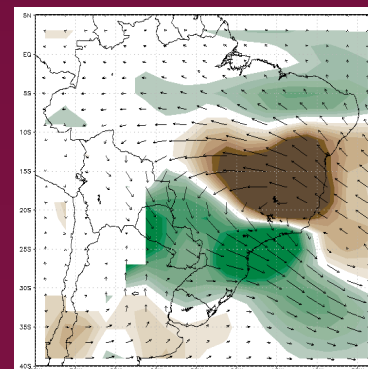
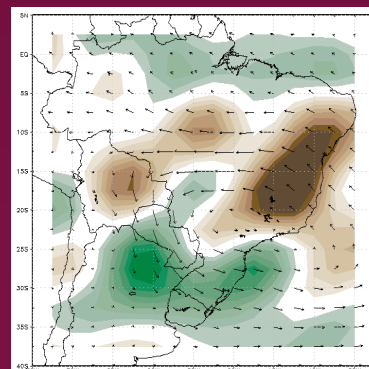
Day -10



Day -5



Day 0



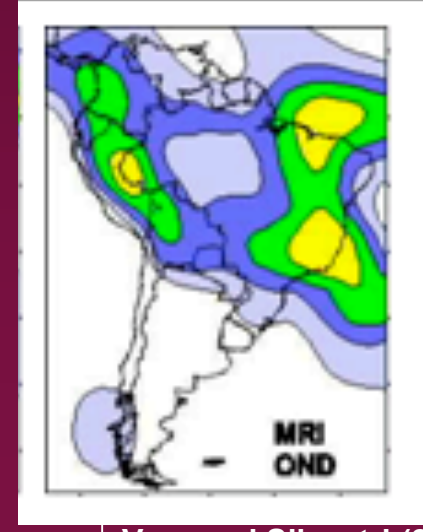
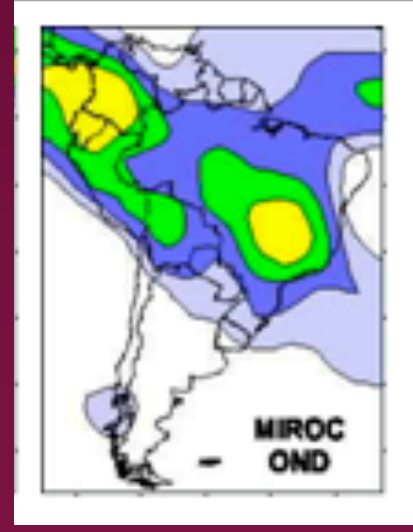
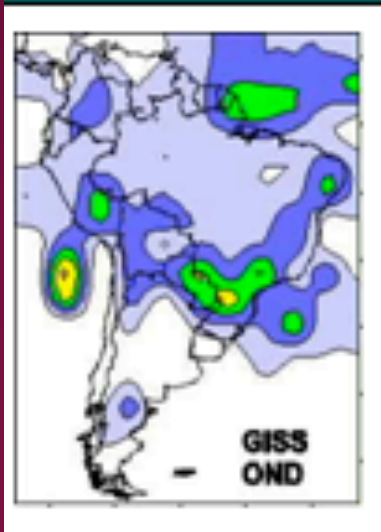
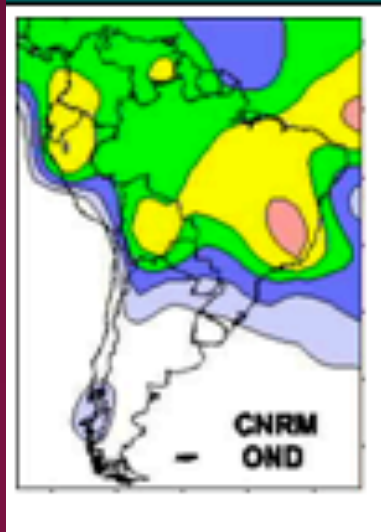
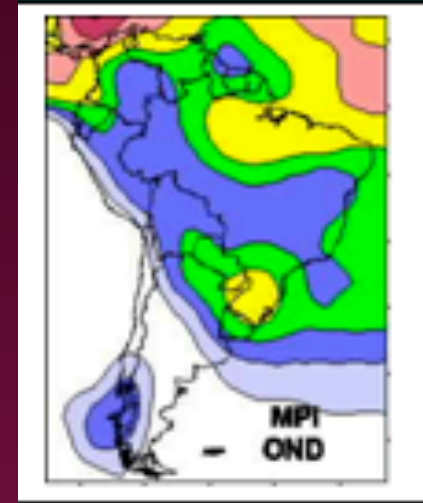
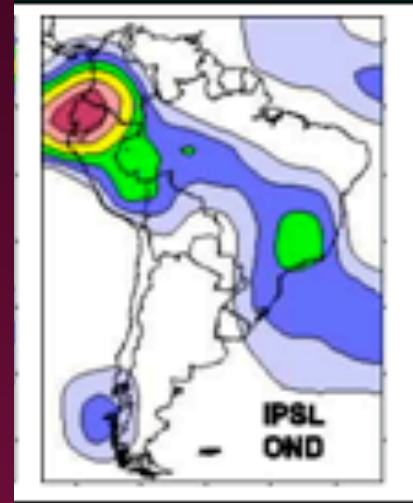
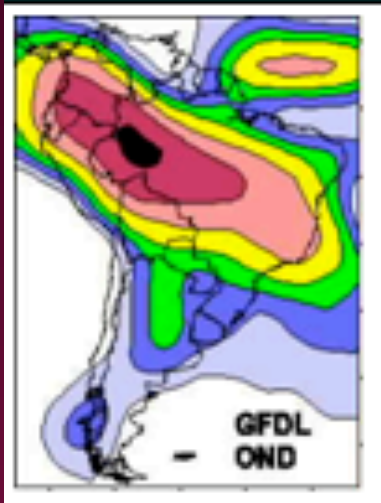
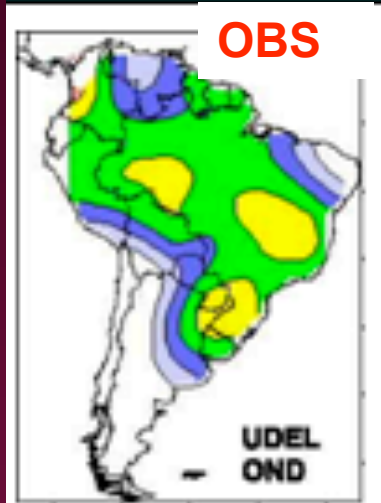
**Regressions
EOF-1 & 850-hPa v'
(Divergence shaded)**

González, Vera, Carril (2007)

Precipitation Interannual Variability

OND (1970-1999)

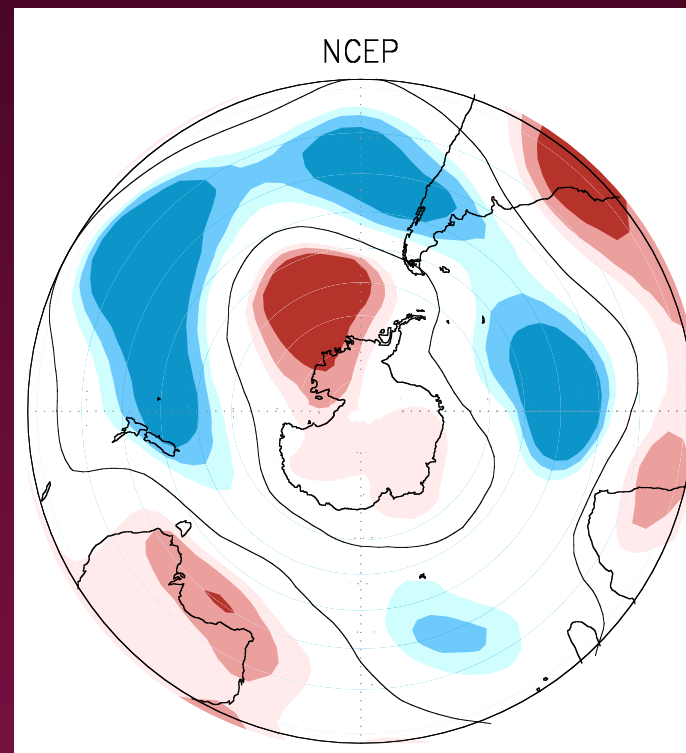
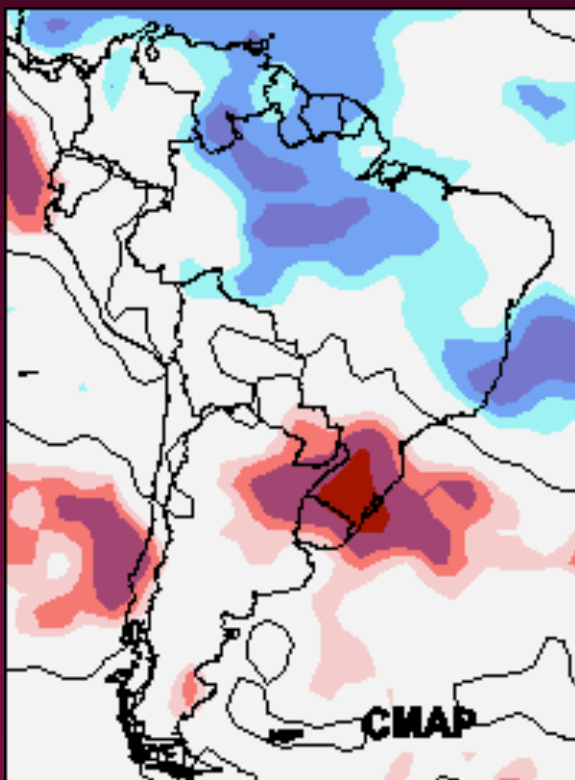
Both ENSO and AAO signature on precipitation variability are largest over La Plata Basin during austral spring



ENSO

OND

(1979-1999)

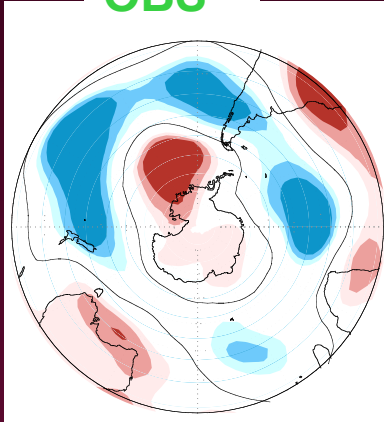


Correlations between El Niño 3.4 SST anomalies and (left) precipitation and (right) 500-hPa geopotential height anomalies. Significant values at 90, 95 and 99% are shaded. NCEP reanalysis data.

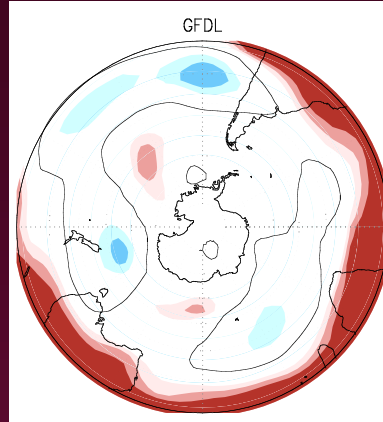
(Vera and Silvestri, 2007)

ENSO signal in SH Circulation anomalies from WCRP/CMIP3 models

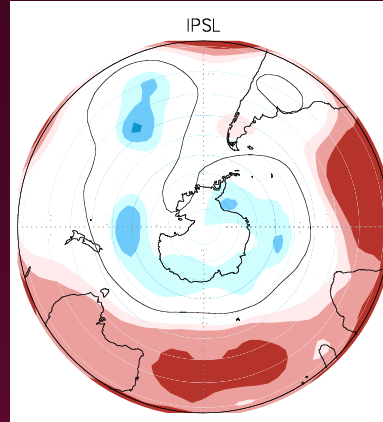
OBS



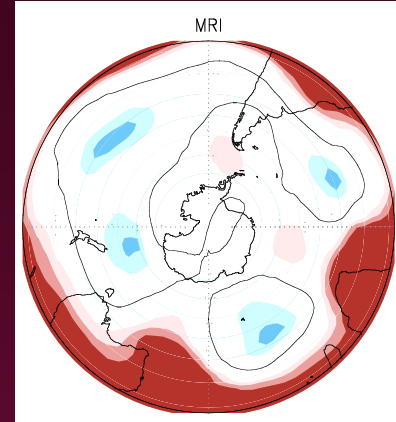
GFDL



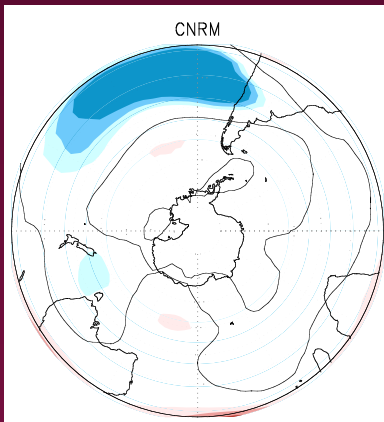
IPSL



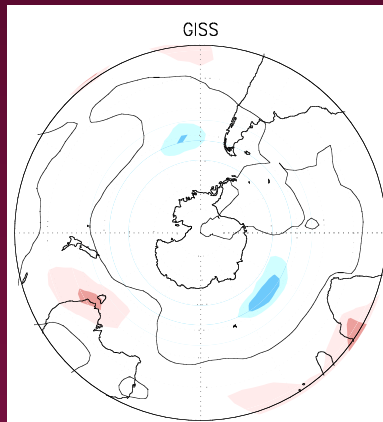
MRI



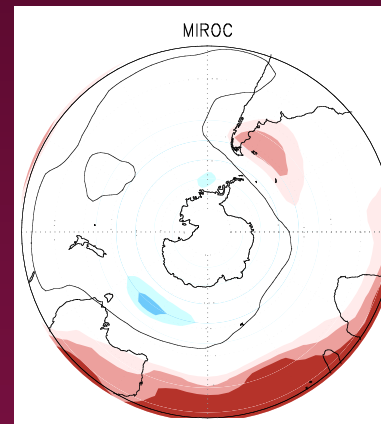
CNRM



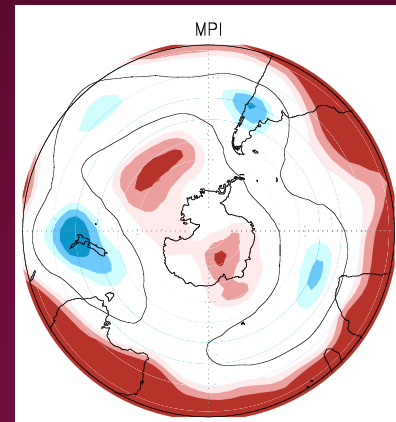
GISS



MIROC



MPI

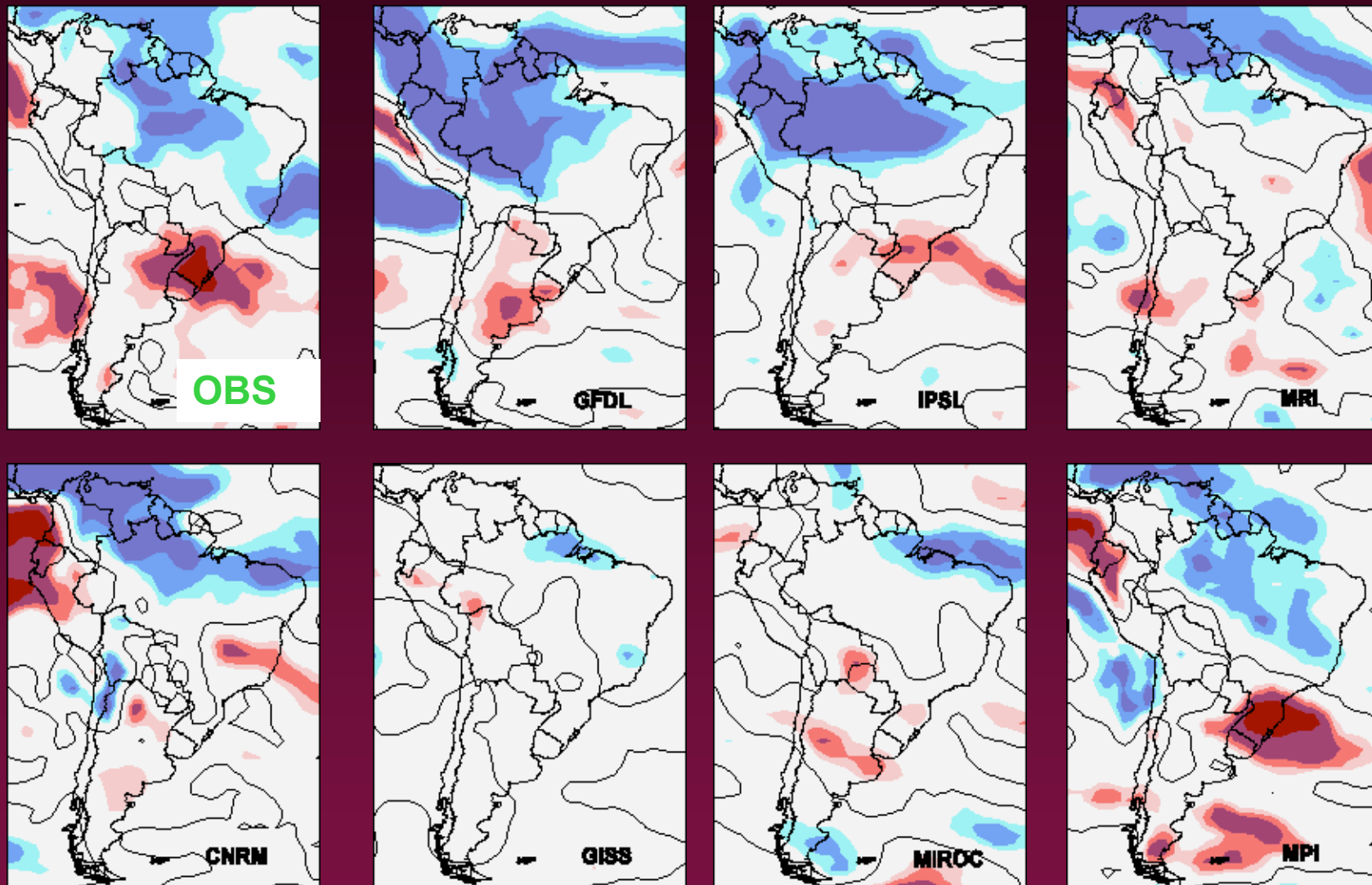


OND (1970-1999)

Correlations between ENSO index and 500-hPa geopotential height anomalies. Significant values at 90, 95 and 99% are shaded.

(Vera and Silvestri 2007)

ENSO signal in South America precipitation anomalies from WCRP/CMIP3 models



OND (1970-1999)

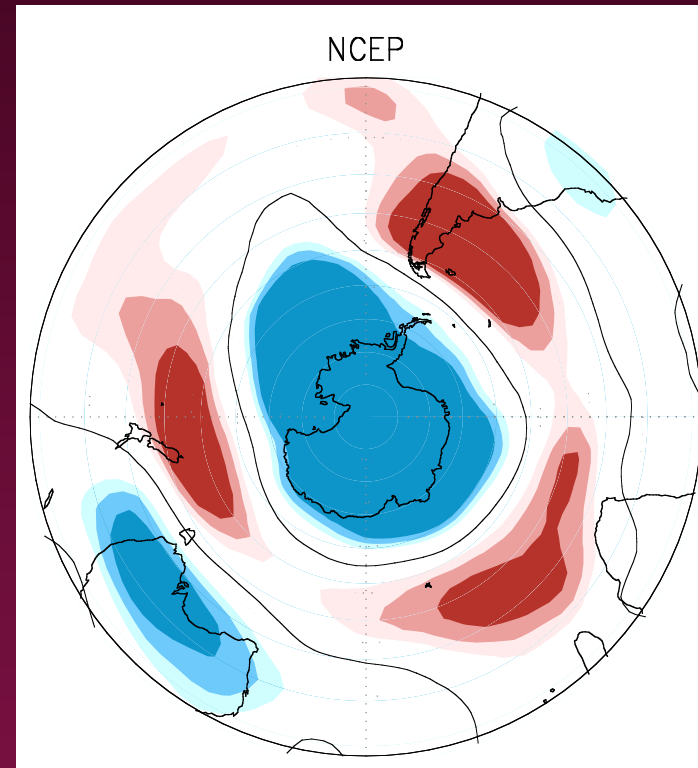
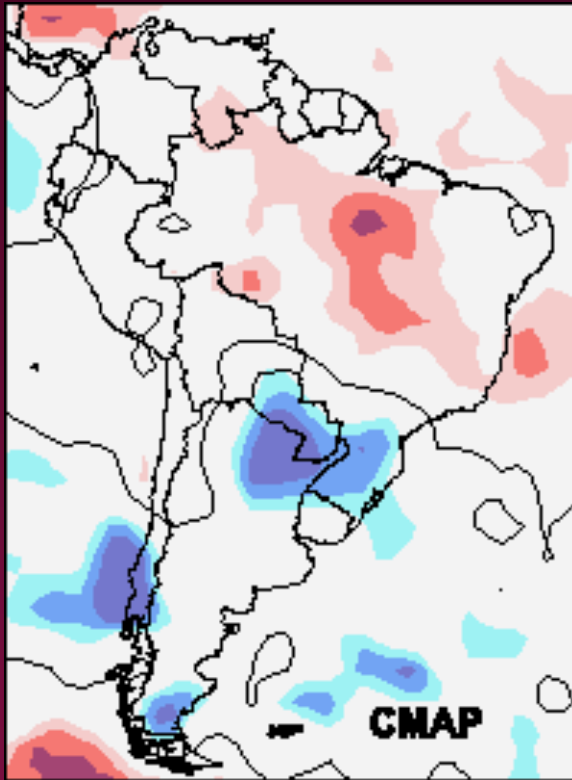
Correlations between ENSO index and precipitation anomalies. Significant values at 90, 95 and 99% are shaded.

(Vera and Silvestri 2007)

Southern Annular Mode (SAM)

OND

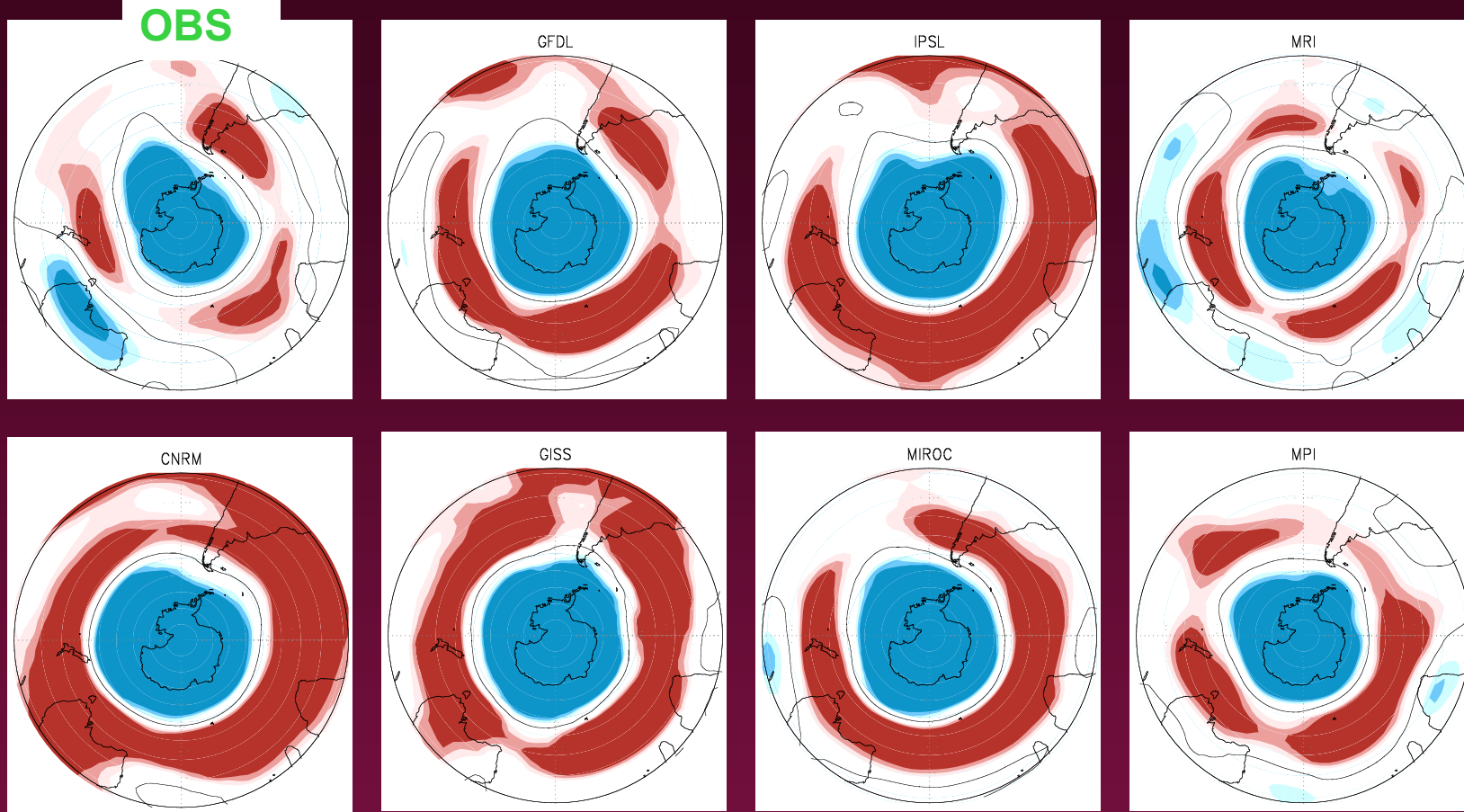
(1979-1999)



Correlations between SAM index and (left) precipitation and (right) 500-hPa geopotential height anomalies. Significant values at 90, 95 and 99% are shaded. NCEP reanalysis data.

(Vera and Silvestri, 2007)

SAM signal in SH circulation anomalies from IPCC-AR4 models

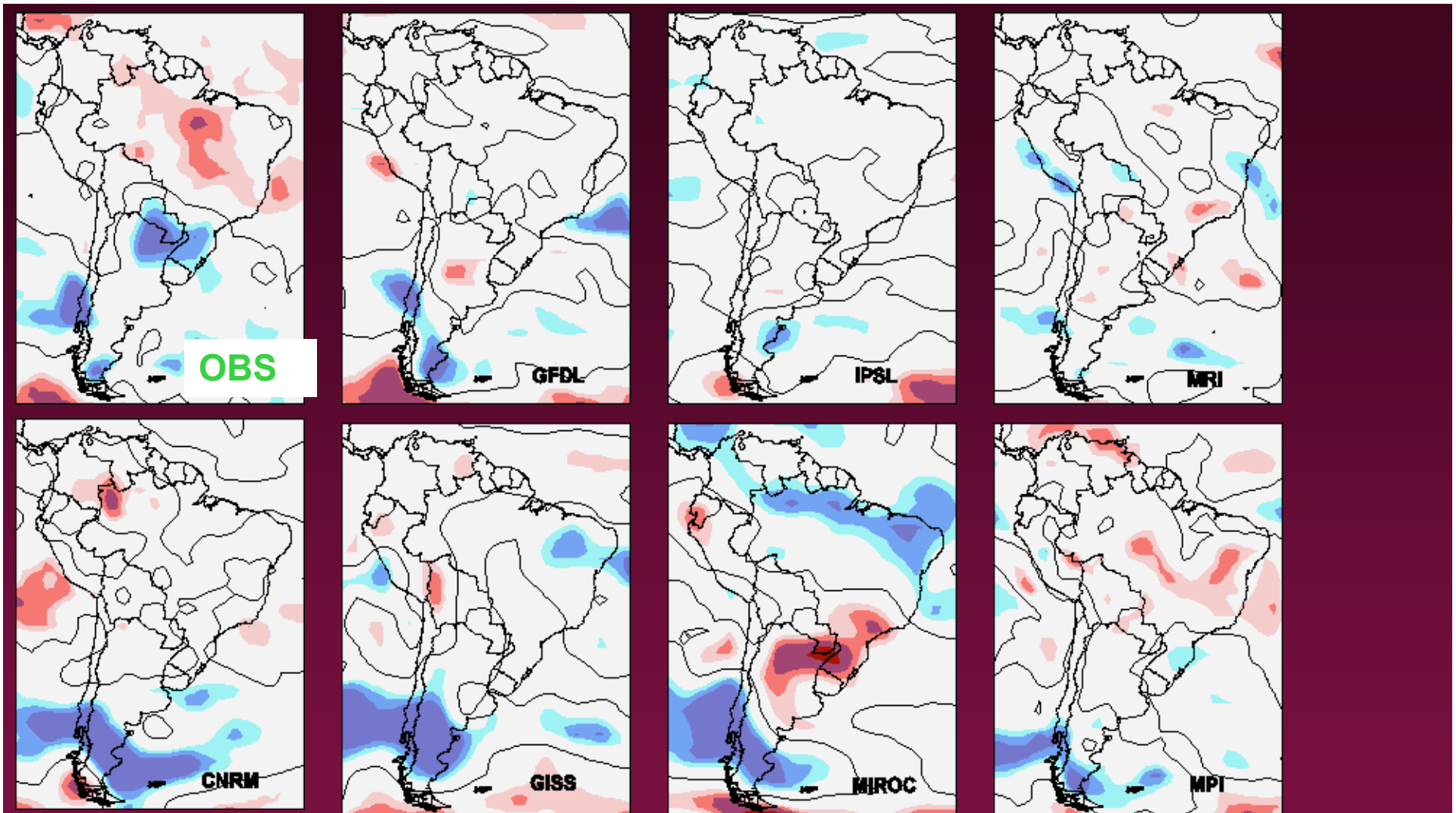


OND (1970-1999)

Correlations between SAM index and 500-hPa geopotential height anomalies. Significant values at 90, 95 and 99% are shaded.

(Vera and Silvestri, 2007)

SAM signal in South America precipitation anomalies from IPCC models



OND (1970-1999)

Correlations between SAM index and 500-hPa geopotential height anomalies. Significant values at 90, 95 and 99% are shaded.

(Vera et al. 2007)

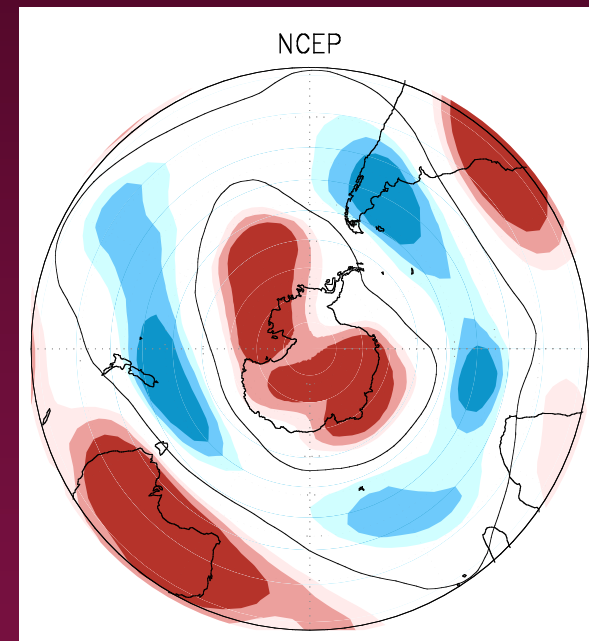
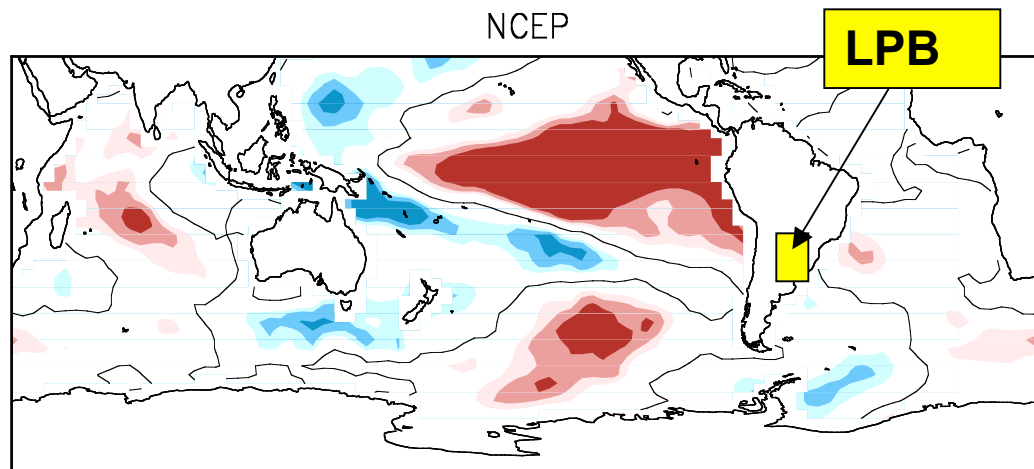
Interannual Variability in the La Plata Basin (LPB)

-ENSO warm events
-SAM negative phase



Positive OND
precipitation
anomalies in LPB

(1970-1999)

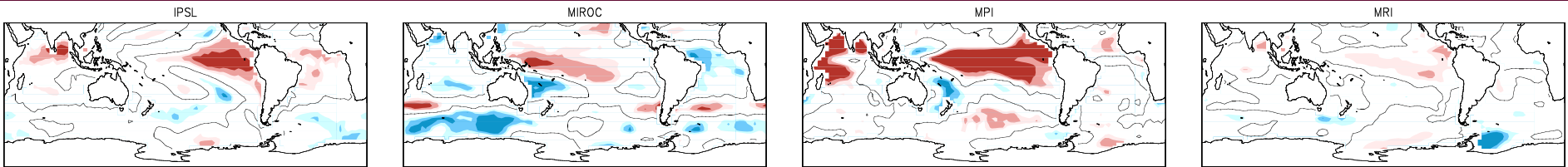
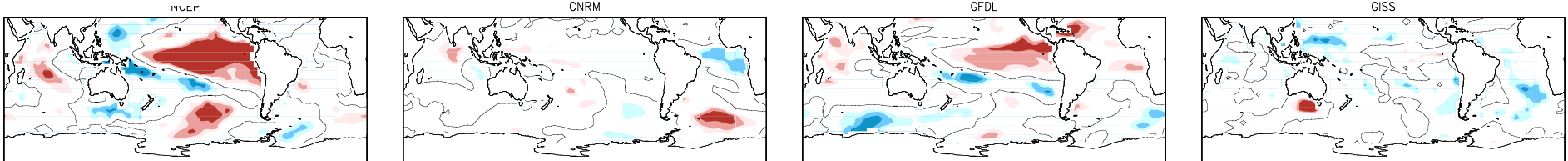


Correlations between precipitation anomalies in LPB and (left) SST anomalies and (right) 500-hPa geopotential height anomalies. Significant values at 90, 95 and 99% are shaded. NCEP reanalysis data.

(Vera and Silvestri 2007)

Correlations between OND precipitation anomalies in LPB and SST anomalies from WCRP/CMIP3 models

OBS

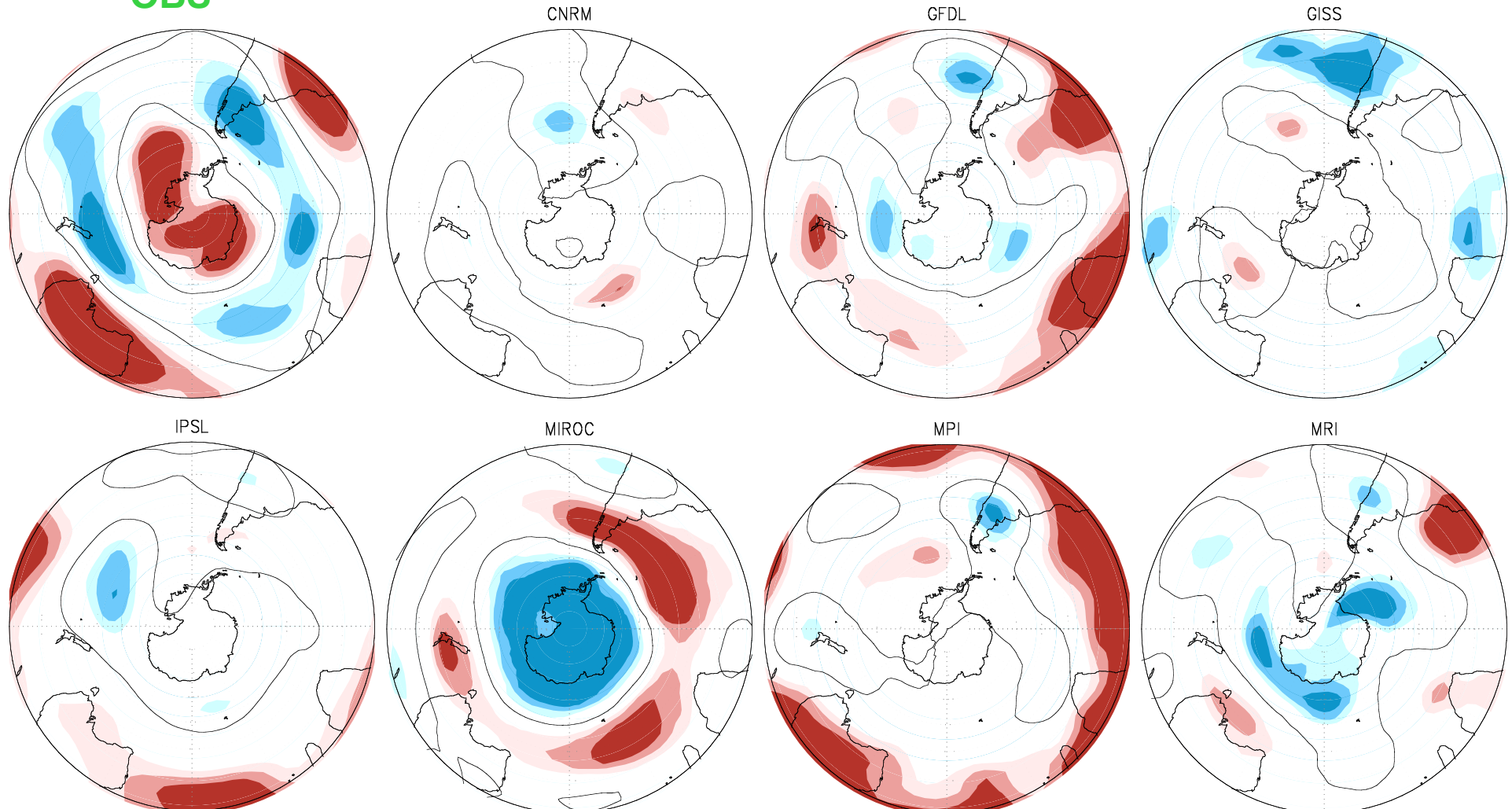


Significant values at 90, 95 and 99% are shaded.

(Vera and Silvestri, 2007)

Correlations between precipitation anomalies in LPB and 500-hPa geopotential height anomalies from WCRP/CMIP3 models

OBS

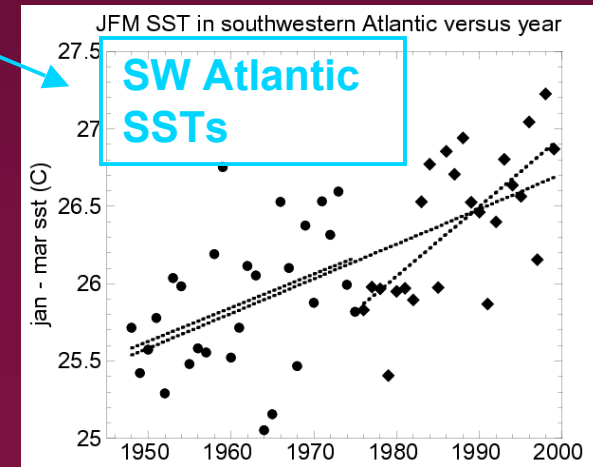
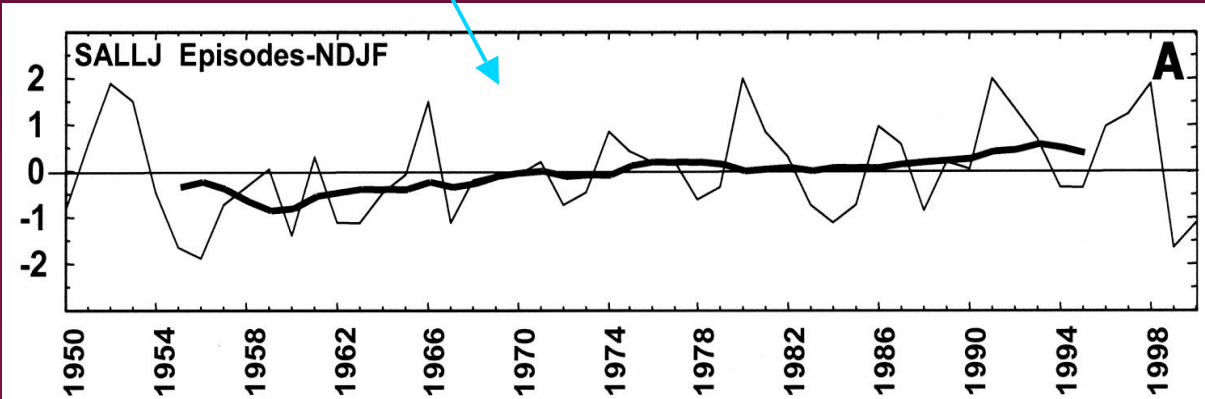
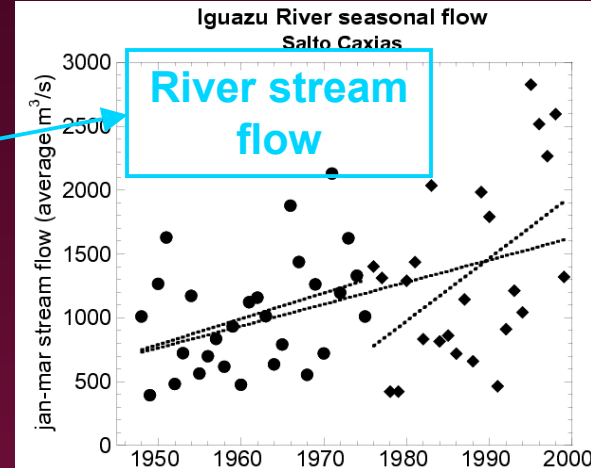
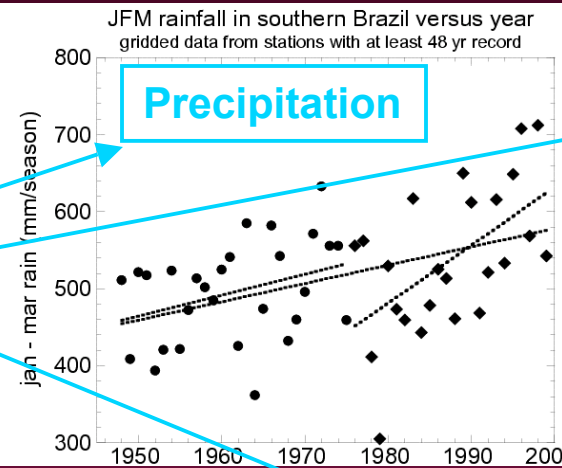
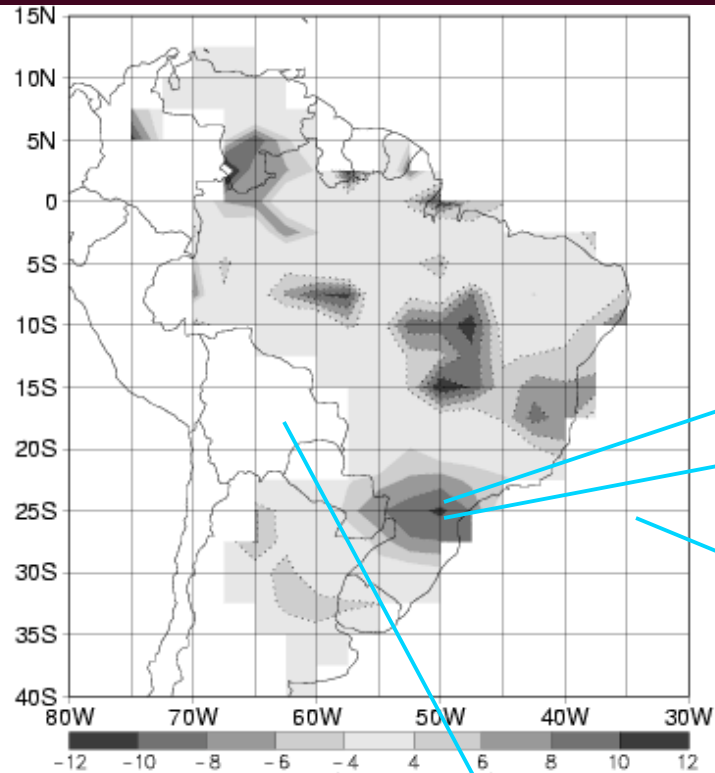


Significant values at 90, 95 and 99% are shaded.

(Vera and Silvestri, 2007)

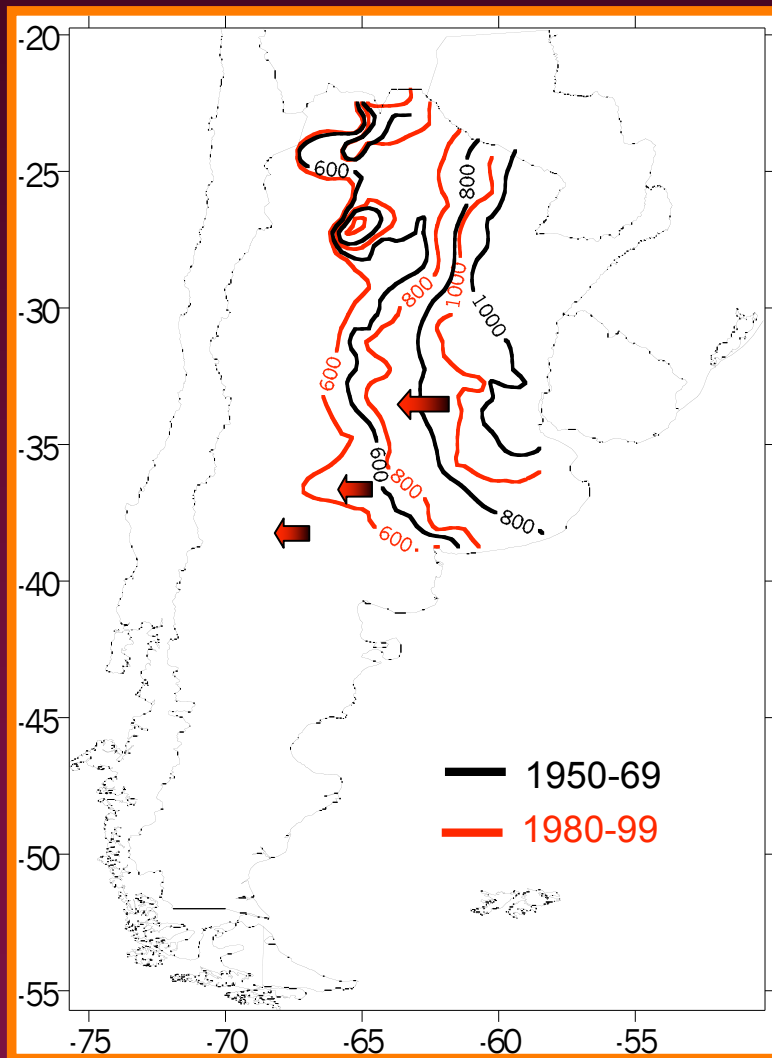
JFM Precipitation Trends observed in LPB

(Liebmann, et al. 2004)



Normalized annual departures of SALLJ-event annual counts

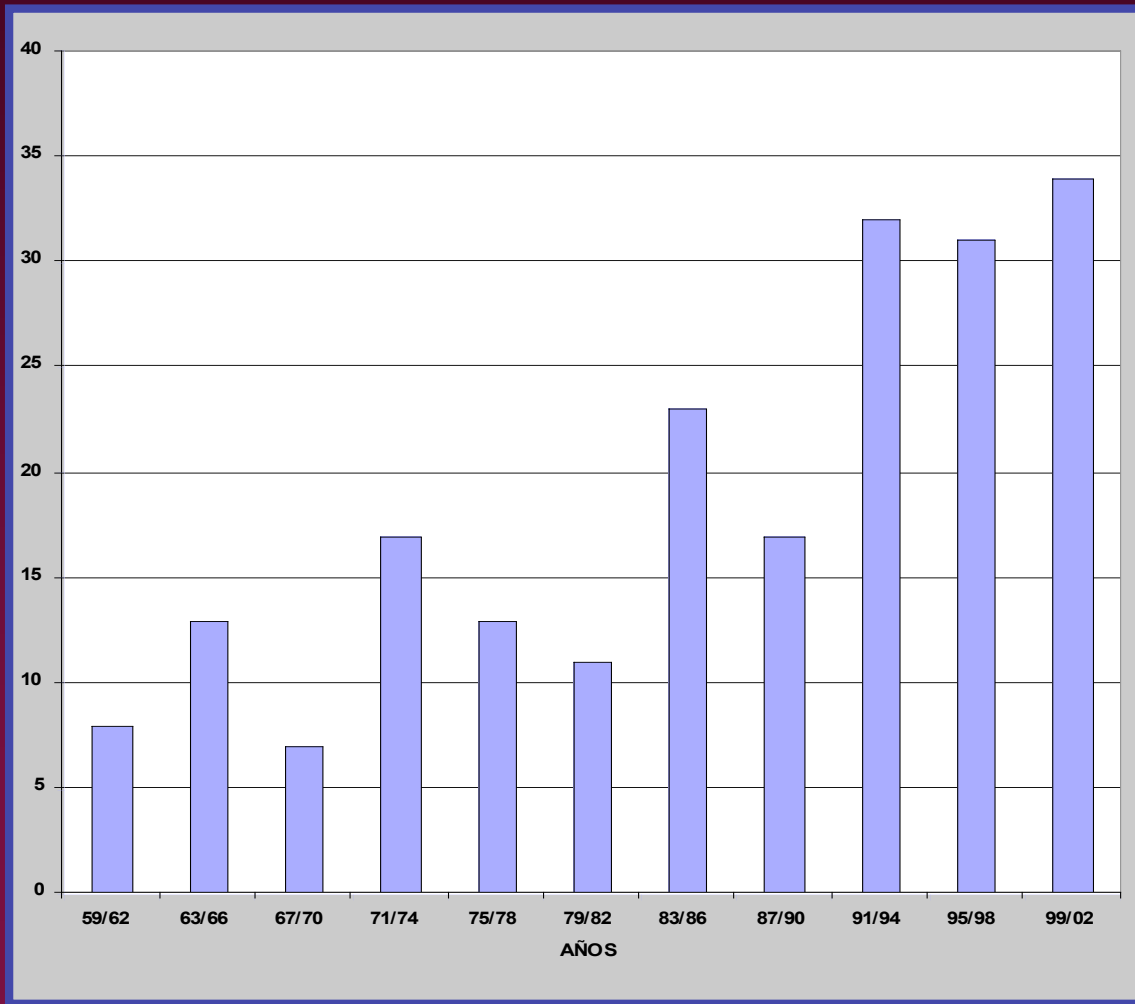
Impacts resulting from precipitation long-term positive trends



Expansion of the agricultural area to the west.

Camilloni et al. (2005)

Observed changes in the extreme precipitation events

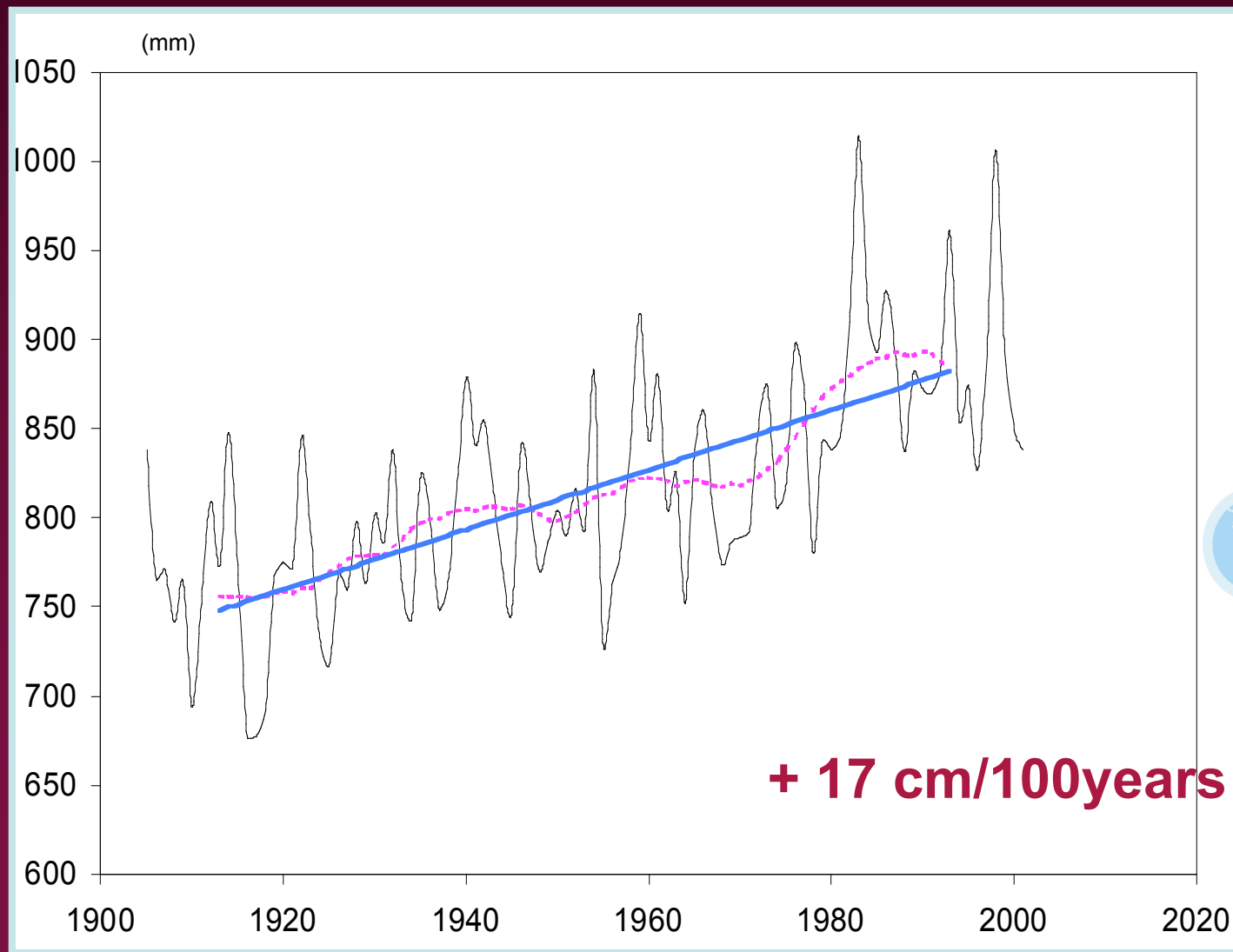


Frequency of 2-daily precipitation events larger than 100 mm over Central and Eastern Argentina.

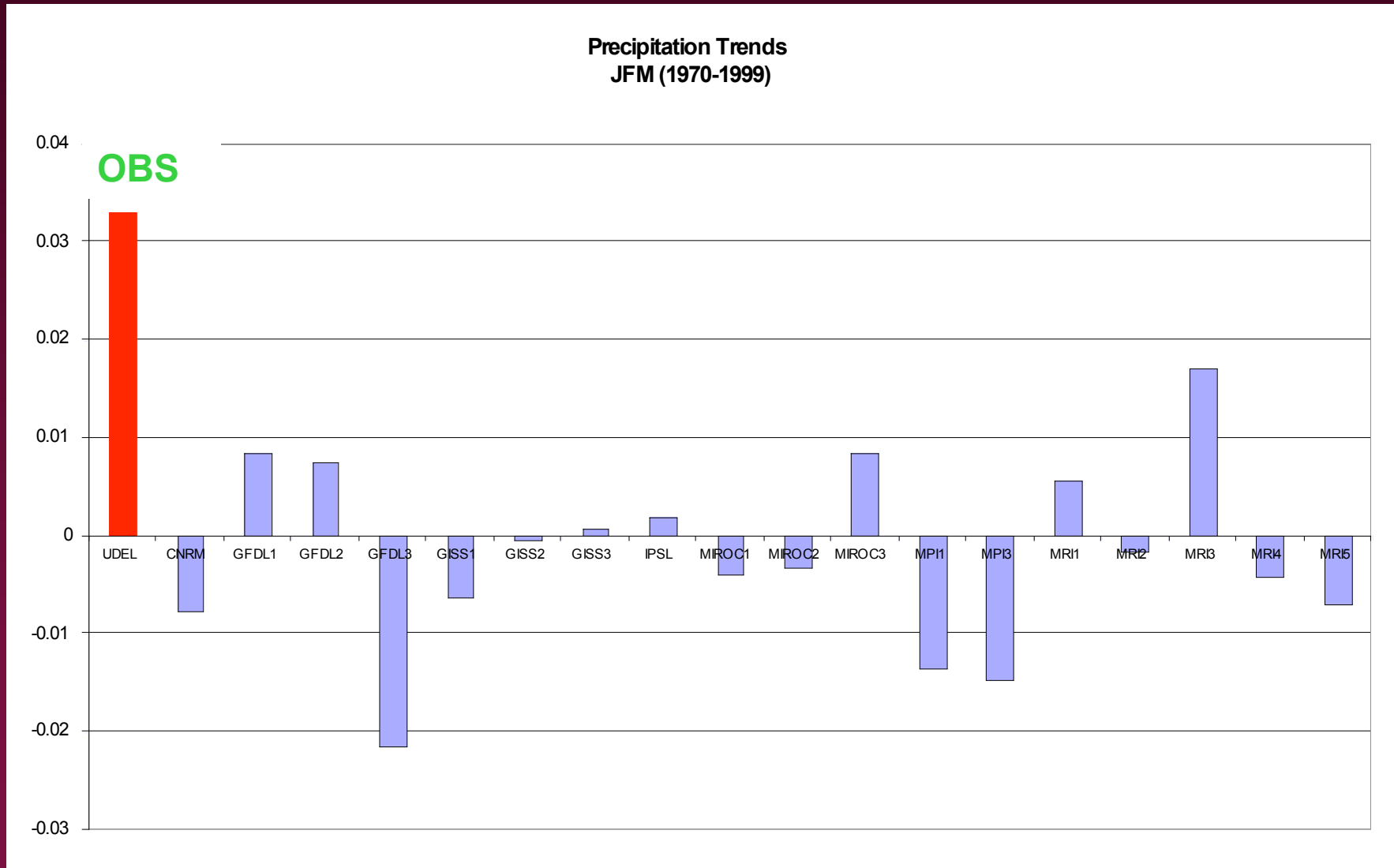
Camilloni et al. (2005)

Changes in the de la Plata river level at Buenos Aires Harbor

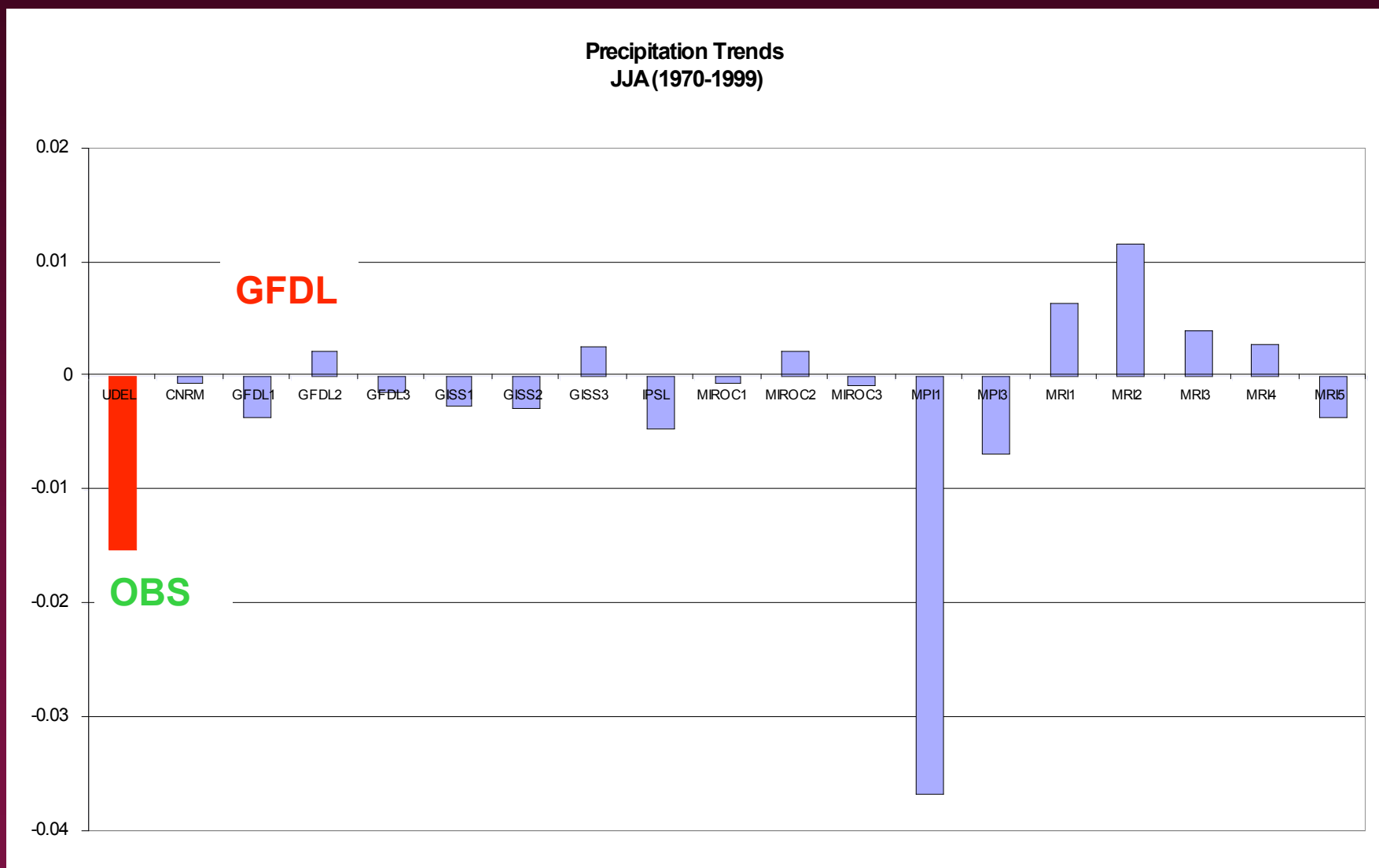
(D'Onofrio, SHN)



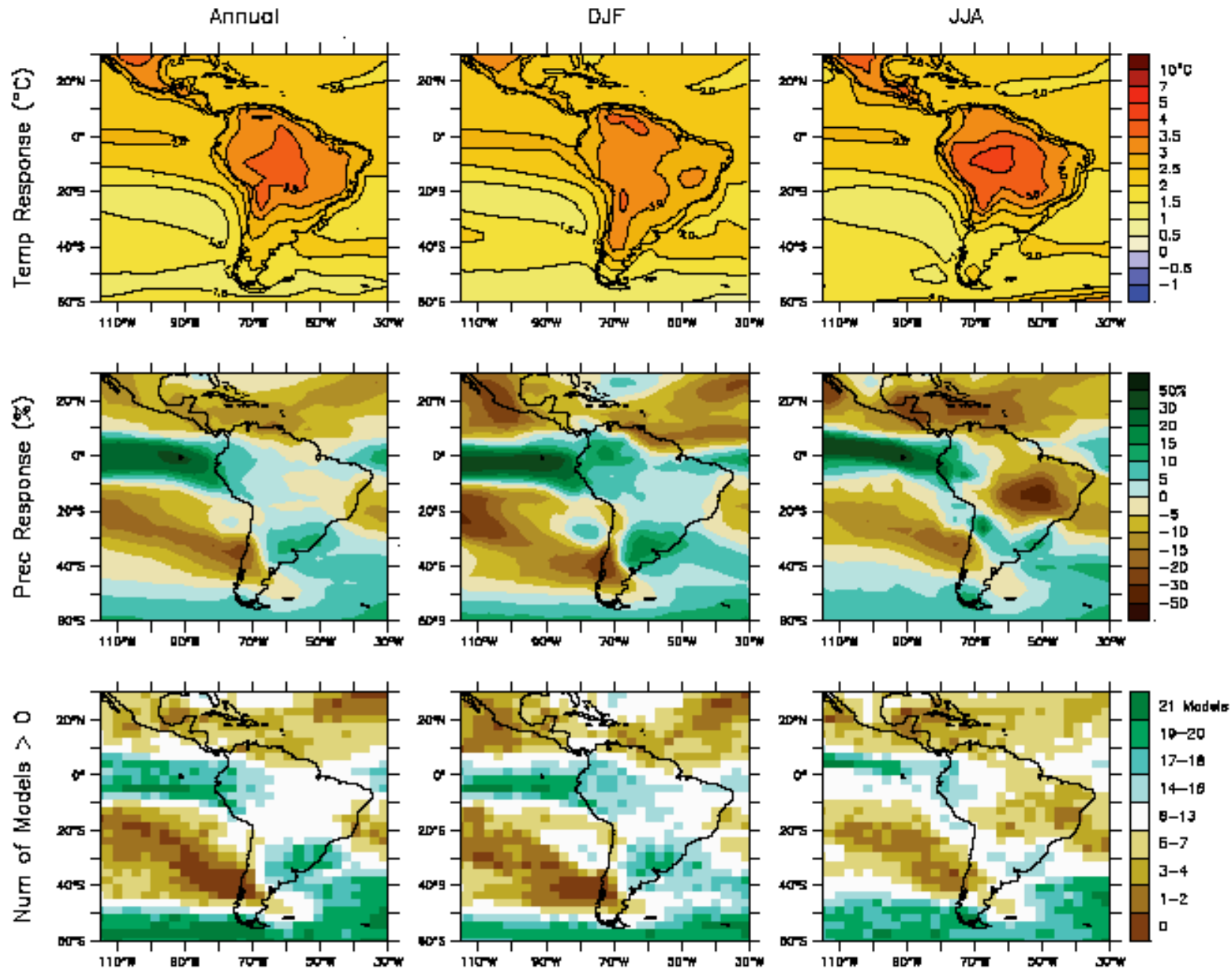
JFM Precipitation Trends in LPB from WCRP/CMIP3 models



JJA Precipitation Trends in LPB from WCRP/CMIP3 models

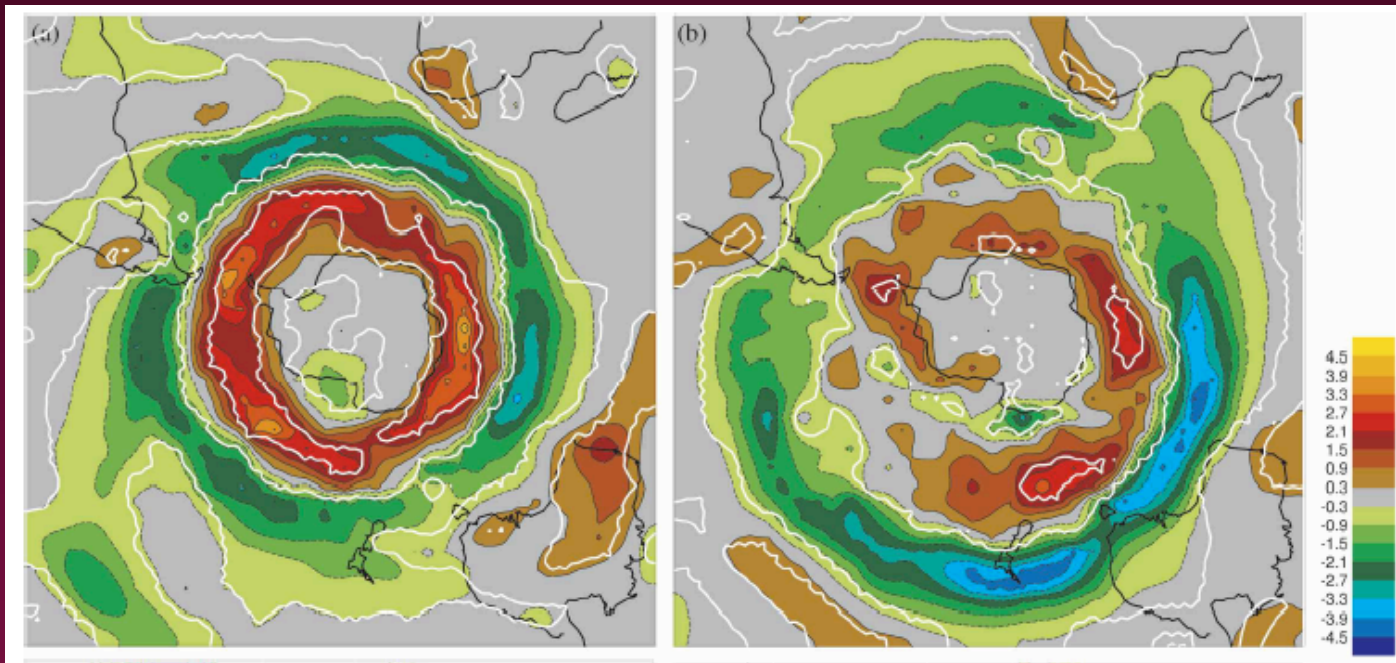


Temperature and precipitation changes from Multi-model ensemble simulations (2080-2099)-(1980-1999). SRES A1B



REDUCTION OF PRECIPITATION IN THE SOUTHERN ANDES:

Poleward shift of the storm tracks



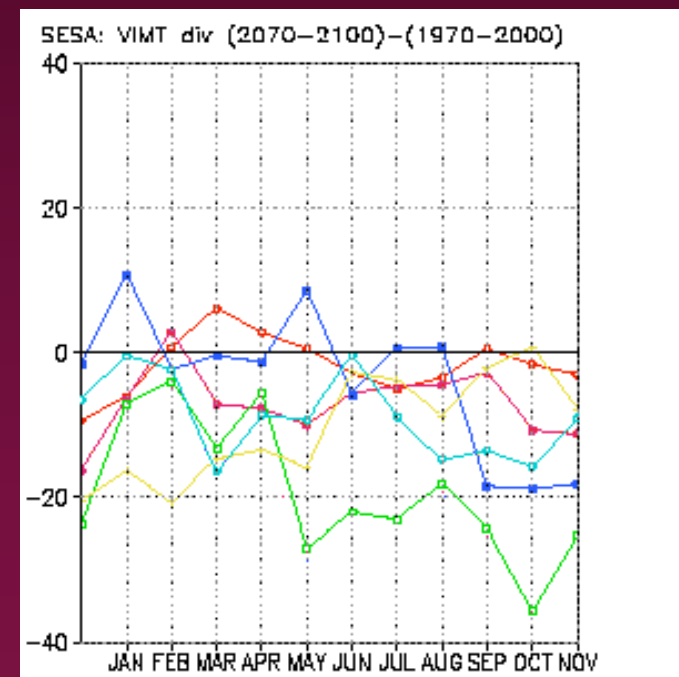
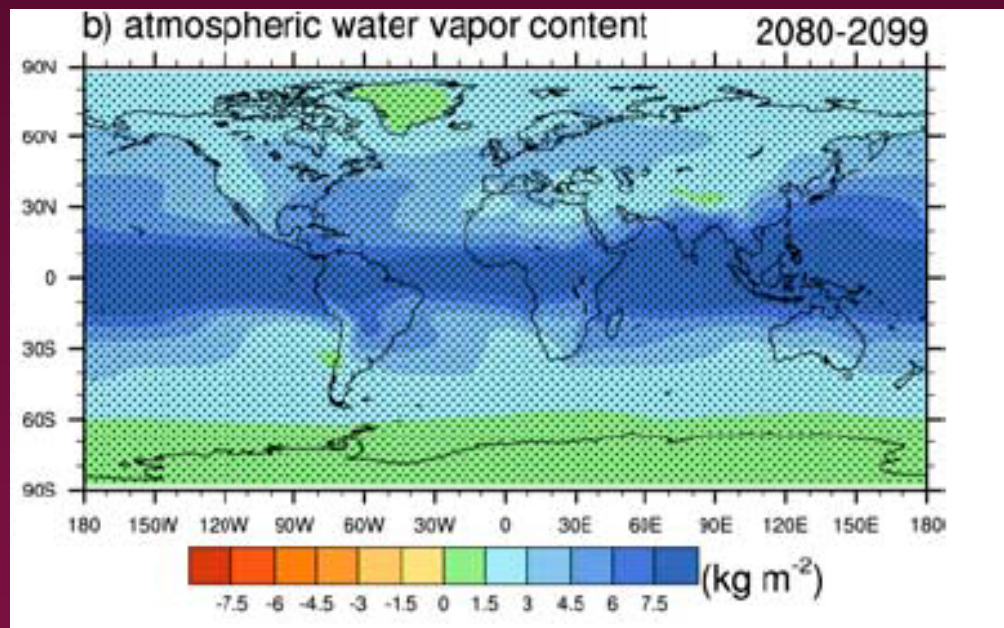
Difference in SH cyclone tracks between the 21C and 20C model simulation (left) DJF track density, (right) JJA track density (Bengtsson et al. 2006)

PRECIPITATION INCREASE IN THE LPB:

Increased tropical SST anomalies → increased water vapor at tropical continental regions → Advective effects (associated with circulation changes)



Increased moisture convergence



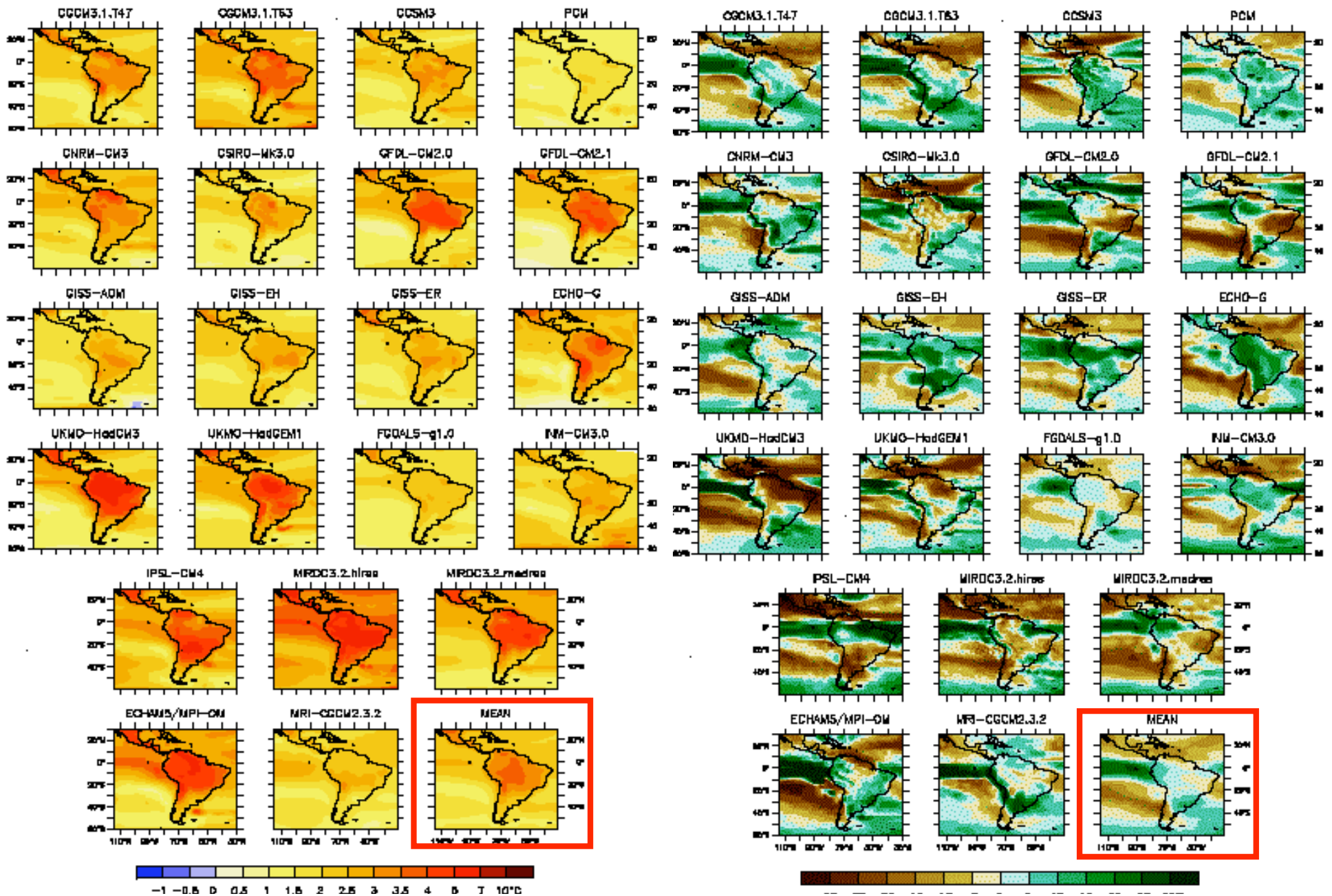
Meehl et al. (2005)

Rojas et al. (2008)

Temperature and precipitation changes (2080-2099)-(1980-1999). SRES A1B

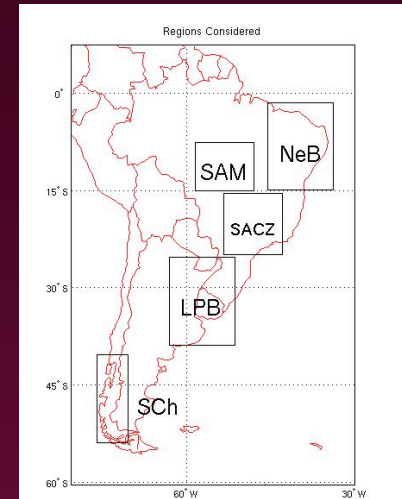
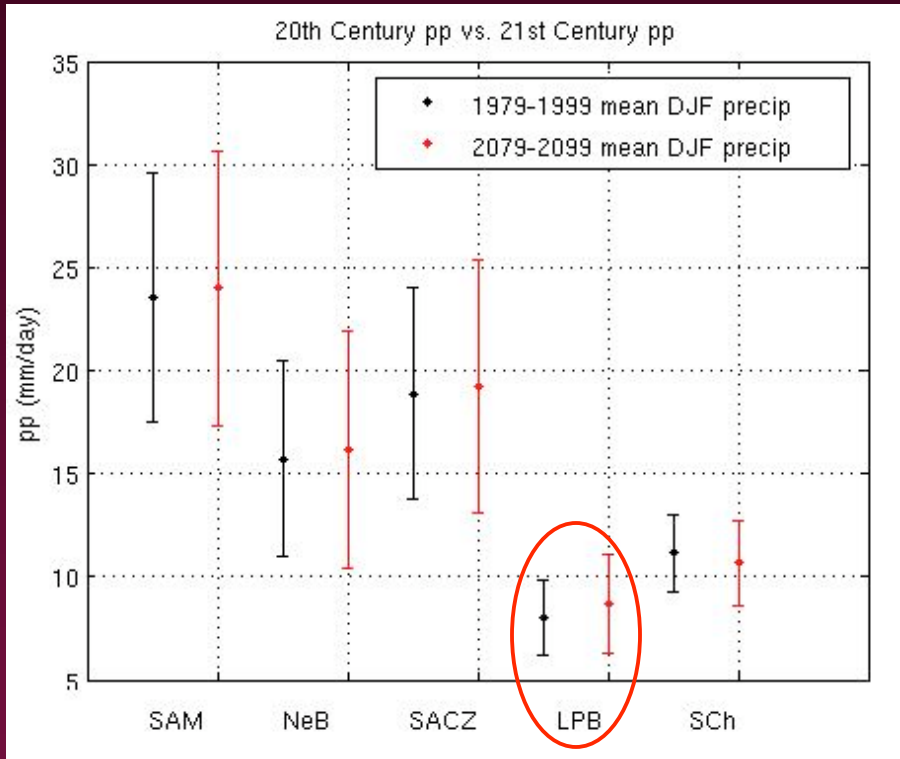
Annual Mean Surface Air Temp Response ($^{\circ}\text{C}$)

Annual Mean Precip Response (%)



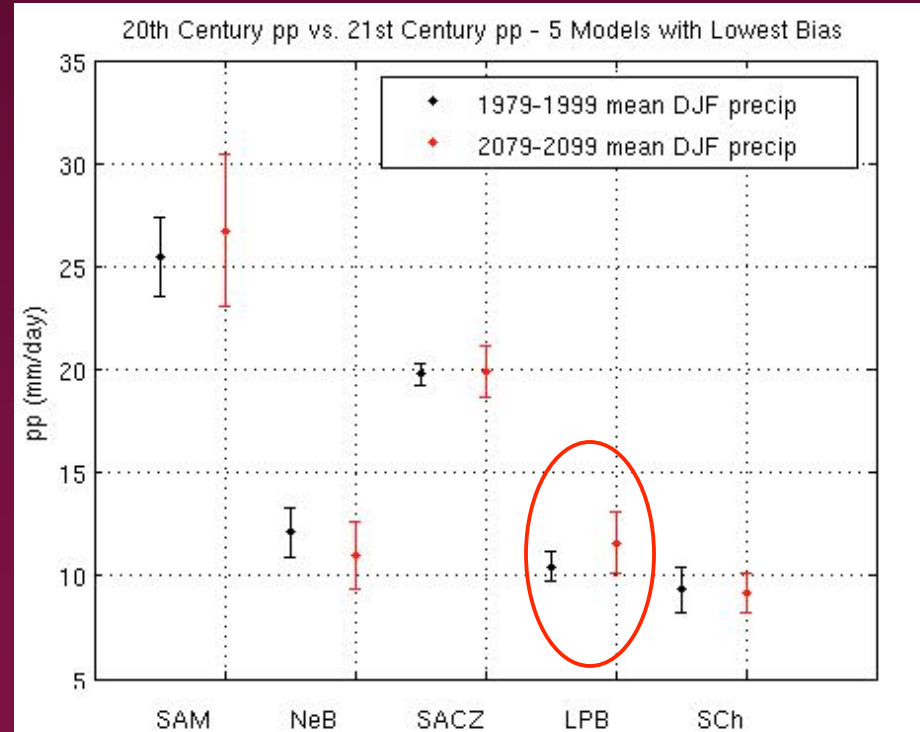
Uncertainties in the DJF precipitation changes from the multi-model ensemble (2080-2099)-(1980-1999). SRES A1B

20 Model simulations



5 Models with lowest Bias

González and Vera (2007)



Modeling Strategy: A multiscale approach

- Deficiencies in the ability to model "local" processes, are among the leading factors limiting forecast skill throughout the American region.
- The relatively poor simulation of some key elements like the diurnal cycle, some aspects of the low level jets, planetary boundary layer processes, clouds and ocean mixing not only require a regional multi-scale focus but also are critical issues for improving global model simulations and predictions.
- Improvements to the physical parameterizations, and improvements to how we model the interactions between the local processes and regional and larger scale variability in regional and global models are needed.

VAMOS Modeling Plan

(www.clivar.org)



- **Integrated Approach**
 - SST Variability in the Pan-American Seas
 - Monsoon Onset, Maturation and Demise
 - Droughts and Floods
 - Diurnal Cycle
- **Cross-Cuts:**
 - Metrics for model assessments
 - Assessment of Models
 - Hypothesis Driven Numerical Experimentation
 - “Climate Process Team” Model Development/ Improvement Strategies
- **Data Assimilation, Analysis and Assessing Observing Systems**
 - To assess the impact of the VAMOS observations, better understand the nature of model errors, and to obtain a better understanding and improved simulation of the full range of phenomena comprising the American monsoon systems.
- **Prediction and Global Scale Linkages**
 - A key issue: To determine the extent to which model improvements made in the simulation of regional-scale phenomena (diurnal cycle, basic monsoon evolution, low level jets, etc), validated against improved data sets, ultimately translate into improved dynamical predictions and more reliable climate change projections.

